

Integrin $\alpha 3 \beta 1$ regulates kidney collecting duct development via TRAF6-dependent K63-linked polyubiquitination of Akt

Eugenia M. Yazlovitskaya^a, Hui-Yuan Tseng^b, Olga Viquez^a, Tianxiang Tu^a, Glenda Mernaugh^a, Karen K. McKee^c, Karen Riggins^a, Vito Quaranta^d, Amrita Pathak^e, Bruce D. Carter^e, Peter Yurchenco^c, Arnoud Sonnenberg^f, Ralph T. Böttcher^b, Ambra Pozzi^{a,d,g}, and Roy Zent^{a,d,g,h}

^aDivision of Nephrology and Hypertension, Department of Medicine, ^dDepartment of Cancer Biology, ^eDepartment of Biochemistry, and ^gDepartment of Cell and Developmental Biology, Vanderbilt University School of Medicine, Nashville, TN 37232; ^bDepartment of Molecular Medicine, Max Planck Institute of Biochemistry, 82152 Martinsried, Germany; ^cDepartment of Pathology and Laboratory Medicine, Robert Wood Johnson Medical School, Piscataway, NJ 08854; ^fDivision of Cell Biology, Netherlands Cancer Institute, 1066 CX Amsterdam, Netherlands; ^hVeterans Affairs Hospital, Nashville, TN 37232

ABSTRACT The collecting system of the kidney develops from the ureteric bud (UB), which undergoes branching morphogenesis, a process regulated by multiple factors, including integrin–extracellular matrix interactions. The laminin (LM)-binding integrin $\alpha 3 \beta 1$ is crucial for this developmental program; however, the LM types and LM/integrin $\alpha 3 \beta 1$ -dependent signaling pathways are poorly defined. We show that $\alpha 3$ chain-containing LMs promote normal UB branching morphogenesis and that LM-332 is a better substrate than LM-511 for stimulating integrin $\alpha 3 \beta 1$ -dependent collecting duct cell functions. We demonstrate that integrin $\alpha 3 \beta 1$ -mediated cell adhesion to LM-332 modulates Akt activation in the developing collecting system and that Akt activation is PI3K independent but requires decreased PTEN activity and K63-linked polyubiquitination. We identified the ubiquitin-modifying enzyme TRAF6 as an interactor with the integrin $\beta 1$ subunit and regulator of integrin $\alpha 3 \beta 1$ -dependent Akt activation. Finally, we established that the developmental defects of TRAF6- and integrin $\alpha 3$ -null mouse kidneys are similar. Thus K63-linked polyubiquitination plays a previously unrecognized role in integrin $\alpha 3 \beta 1$ -dependent cell signaling required for UB development and may represent a novel mechanism whereby integrins regulate signaling pathways.

Monitoring Editor

Mark H. Ginsberg
University of California,
San Diego

Received: Jul 10, 2014

Revised: Mar 17, 2015

Accepted: Mar 17, 2015

This article was published online ahead of print in MBoC in Press (<http://www.molbiolcell.org/cgi/doi/10.1091/mbc.E14-07-1203>) on March 25, 2015.

Address correspondence to: Roy Zent (roy.zent@vanderbilt.edu).

Abbreviations used: BrdU, 5-bromodeoxyuridine; CD, collecting duct; DMSO, dimethyl sulfoxide; FAK, focal adhesion kinase; GFP, green fluorescent protein; HA, hemagglutinin; H&E, hematoxylin and eosin; IgG, immunoglobulin G; LM, laminin; PBS, phosphate-buffered saline; PDK1, phosphoinositide-dependent kinase 1; PI3K, phosphoinositide 3-kinase; PIP₂, PI(4,5)P₂; PIP₃, PI(3,4,5)P₃; siRNA, small interfering RNA; TNF, tumor necrosis factor; TRAF6, TNF receptor-associated factor 6; UB, ureteric bud; WT, wild type.

© 2015 Yazlovitskaya et al. This article is distributed by The American Society for Cell Biology under license from the author(s). Two months after publication it is available to the public under an Attribution–Noncommercial–Share Alike 3.0 Unported Creative Commons License (<http://creativecommons.org/licenses/by-nc-sa/3.0>).

“ASCB®,” “The American Society for Cell Biology®,” and “Molecular Biology of the Cell®” are registered trademarks of The American Society for Cell Biology.

INTRODUCTION

The kidney develops from two distinct embryonic components: the ureteric bud (UB), which forms the multibranching collecting system, and the metanephric mesenchyme, which gives rise to the nephrons. The formation of the collecting system occurs by iterative branching morphogenesis of the UB, a process regulated by multiple factors, including integrin-dependent cell–extracellular matrix (ECM) interactions.

Laminins (LMs), trimeric proteins consisting of α , β , and γ chains, are the principal ECM components that regulate UB development. There are five α chains, four β chains, and three γ chains, which can form 15 LM trimers (Aumailley et al., 2005). The $\gamma 1$, $\alpha 5$, and $\alpha 3$ LM chains are expressed in UB-derived structures (Zent et al., 2001;

Chen *et al.*, 2004; Miner and Yurchenco, 2004). The $\gamma 1$ chain, found in 10 of the LMs, is critical for UB development, as mice lacking this chain in the UB have a severe kidney branching morphogenesis defect (Yang *et al.*, 2011). The LM $\alpha 5$ chain, found in LM-511 and LM-521, is also necessary for normal UB development, as LM $\alpha 5$ -null mice have a mild branching morphogenesis defect (Liu *et al.*, 2009). The role of the $\alpha 3$ chain-containing LMs (LM-332, LM-321, and LM-311) in UB development *in vivo* is less well defined, as their importance in branching morphogenesis has only been shown utilizing LM-332 inhibitory antibodies in an *ex vivo* organ culture model (Zent *et al.*, 2001).

Integrins are heterodimeric transmembrane matrix receptors consisting of $\alpha\beta$ subunits that exhibit different ligand-binding properties. Twenty-four integrins are found in mammals, and four of them— $\alpha 3\beta 1$, $\alpha 6\beta 1$, $\alpha 6\beta 4$, and $\alpha 7\beta 1$ —primarily bind to LMs. While integrins $\alpha 3\beta 1$, $\alpha 6\beta 1$, and $\alpha 6\beta 4$ are expressed in the developing UB (Zent *et al.*, 2001), integrin $\alpha 3\beta 1$ is the major receptor that mediates UB formation (Liu *et al.*, 2009). The global integrin $\alpha 3$ -null mouse, which dies at birth, presents with an abnormal renal papilla outgrowth evident at embryonic day 18.5 (E18.5; Kreidberg *et al.*, 1996). Specific deletion of the integrin $\alpha 3$ subunit in the UB using the *Hoxb7Cre/green fluorescent protein (GFP)* mouse results in adult mice with absent or dramatically flattened papillae (Liu *et al.*, 2009). This abnormality was proposed to be due to alterations in expression of *Wnt7b* and *Wnt4* *in vivo* (Liu *et al.*, 2009). Integrin $\alpha 3\beta 1$ -dependent phosphoinositide 3-kinase (PI3K)/Akt signaling was shown to control expression of Wnts in collecting duct (CD) cells, suggesting this signaling pathway modulates Wnts in UB development (Liu *et al.*, 2009). However, the mechanism whereby integrin $\alpha 3\beta 1$ regulates the Akt signaling pathway is currently unknown.

The PI3K/Akt pathway, which plays a central role in multiple biological functions, is stimulated downstream of numerous cell receptors, including growth factor receptors and integrins. Activation of this pathway is complex. PI3K phosphorylates $PI(4,5)P_2$ (PIP₂) to form $PI(3,4,5)P_3$ (PIP₃), which is required for the recruitment of Akt from the cytosol to the plasma membrane (Cantley, 2002). The dual-specificity protein phosphatase PTEN negatively regulates this process by dephosphorylating PIP₃ to PIP₂ (Song *et al.*, 2012). Src-induced phosphorylation of Akt at Tyr315/Tyr326 is required to precondition Akt for membrane binding (Jiang and Qiu, 2003). At the membrane, Akt is phosphorylated on Thr308 within its catalytic domain by phosphoinositide-dependent kinase 1 (PDK1) and at Ser473 within its C-terminal regulatory domain by mammalian target of rapamycin complex 2 (mTORC2), resulting in its full activation (Guertin and Sabatini, 2007; Bayascas, 2008).

A less well-recognized mechanism of regulation of Akt activity is polyubiquitination. Specifically, K63-linked polyubiquitination, executed by the E3 ligase tumor necrosis factor (TNF) receptor-associated factor 6 (TRAF6), promotes Akt translocation to the membrane and is essential for Akt phosphorylation (Yang *et al.*, 2009, 2010). Of the six known TRAF proteins, TRAF6 has several unique features that contribute to its diverse physiological functions. Unlike other TRAFs, which mediate signaling only from the TNF receptor superfamily, TRAF6 also participates in signal transduction from the Toll-like receptor/interleukin-1 receptor superfamily (Wu and Arron, 2003) and other receptors, including TGF- β receptors (Landstrom, 2010). TRAF6 induces K63-linked polyubiquitination of itself and downstream signaling molecules (Wang *et al.*, 2012). It is unclear how the K63-linked polyubiquitination of Akt results in its recruitment to the plasma membrane and its subsequent activation. Moreover, the role of TRAF6-mediated K63-linked polyubiquitination in integrin-dependent signaling is undefined.

The contribution of integrin $\alpha 3\beta 1$ to the development of the kidney collecting system has been investigated; however, the involvement of its LM substrates and the signaling pathways mediated by LM/ $\alpha 3\beta 1$ integrin interactions are poorly defined. In this study, we show that the $\alpha 3$ chain-containing LMs is essential for normal UB branching morphogenesis. We also demonstrate that integrin $\alpha 3\beta 1$ mediates renal CD cell functions by activating Akt via a mechanism that is PI3K independent but requires K63-linked polyubiquitination. Finally, we show that the ubiquitin ligase TRAF6 interacts with the integrin $\beta 1$ subunit and regulates integrin-dependent Akt activation. Thus we conclude that K63-linked polyubiquitination plays a previously unrecognized role in regulating integrin $\alpha 3\beta 1$ -dependent cell signaling that is required for UB development.

RESULTS

The LM $\alpha 3$ chain is required for normal UB development

The $\gamma 1$ and $\alpha 5$ LM chains have been shown to be required for normal UB development *in vivo* (Liu *et al.*, 2009; Yang *et al.*, 2011); however, the role for the $\alpha 3$ -containing LMs is undefined. We previously showed that LM-332 is expressed in early development of the rat UB (Zent *et al.*, 2001). We verified that $\alpha 3$ -containing LMs are expressed in the developing mouse UB in E15 and E19 mouse kidneys by performing immunohistochemistry with antibodies directed against the LM $\alpha 3$ chain, found in LM-311, LM-321, and LM-332, and the LM $\gamma 2$ chain that is specific for LM-332 (Figure 1, A–D). We subsequently defined the role of LM $\alpha 3$ chain in UB development by examining kidneys of LM $\alpha 3$ -null mice, which die at birth due to a skin-blistering condition, on an undefined background, (Ryan *et al.*, 1999). We found that 40% of these mice (12/30) had developed one kidney when examined at birth (postnatal day 1 [P1]). This phenotype was lost as the mice were bred onto a pure C57/Bl6 background. However, examination of embryonic kidneys of LM $\alpha 3$ -null mice on this background revealed mild hypoplasia/dysplasia of the papilla at E18 (Figure 1, E and F), which became more evident in newborn mice (Figure 1, G and H) and is manifested by fewer but more dilated tubules in the papilla. LM $\alpha 3$ deletion also significantly decreased tubule proliferation in the papilla (Figure 1, I–K), suggesting that a proliferative defect accounts in part for the abnormal phenotype. Thus $\alpha 3$ -containing LMs appear to play a distinct role in UB development *in vivo*.

Deleting the integrin $\alpha 3$ subunit in the UB causes branching morphogenesis defects and renal papilla dysplasia/hypoplasia and impairs Akt and p38 MAPK signaling

Deletion of the $\beta 1$ integrin subunit in the UB results in a severe branching morphogenesis defect *in vivo* (Zhang *et al.*, 2009), and organ culture experiments predicted that integrin $\alpha 3\beta 1$ is a major contributor to UB development (Zent *et al.*, 2001). However, when the integrin $\alpha 3$ subunit was specifically deleted in the UB using the *Hoxb7Cre* mouse, only a mild to moderate CD defect characterized by absence or flattening of the papilla was noted (Liu *et al.*, 2009). Owing to this discrepant result, we used *Hoxb7Cre;Itg $\alpha 3^{flox/flox}$* mice that were generated using different targeting strategies (Kobayashi *et al.*, 2005; Sachs *et al.*, 2006) to those published (Liu *et al.*, 2009; see *Materials and Methods* for details). These mice had a normal lifespan despite complete deletion of the integrin $\alpha 3$ subunit in the UB (Figure 2M). The kidneys had a mild UB branching morphogenesis defect that was first evident at E15 (Figure 2, A and B). At E18 and P1, the papillae of kidneys from *Hoxb7Cre;Itg $\alpha 3^{flox/flox}$* mice were hypoplastic/dysplastic with fewer and more dilated CDs when compared with kidneys from controls

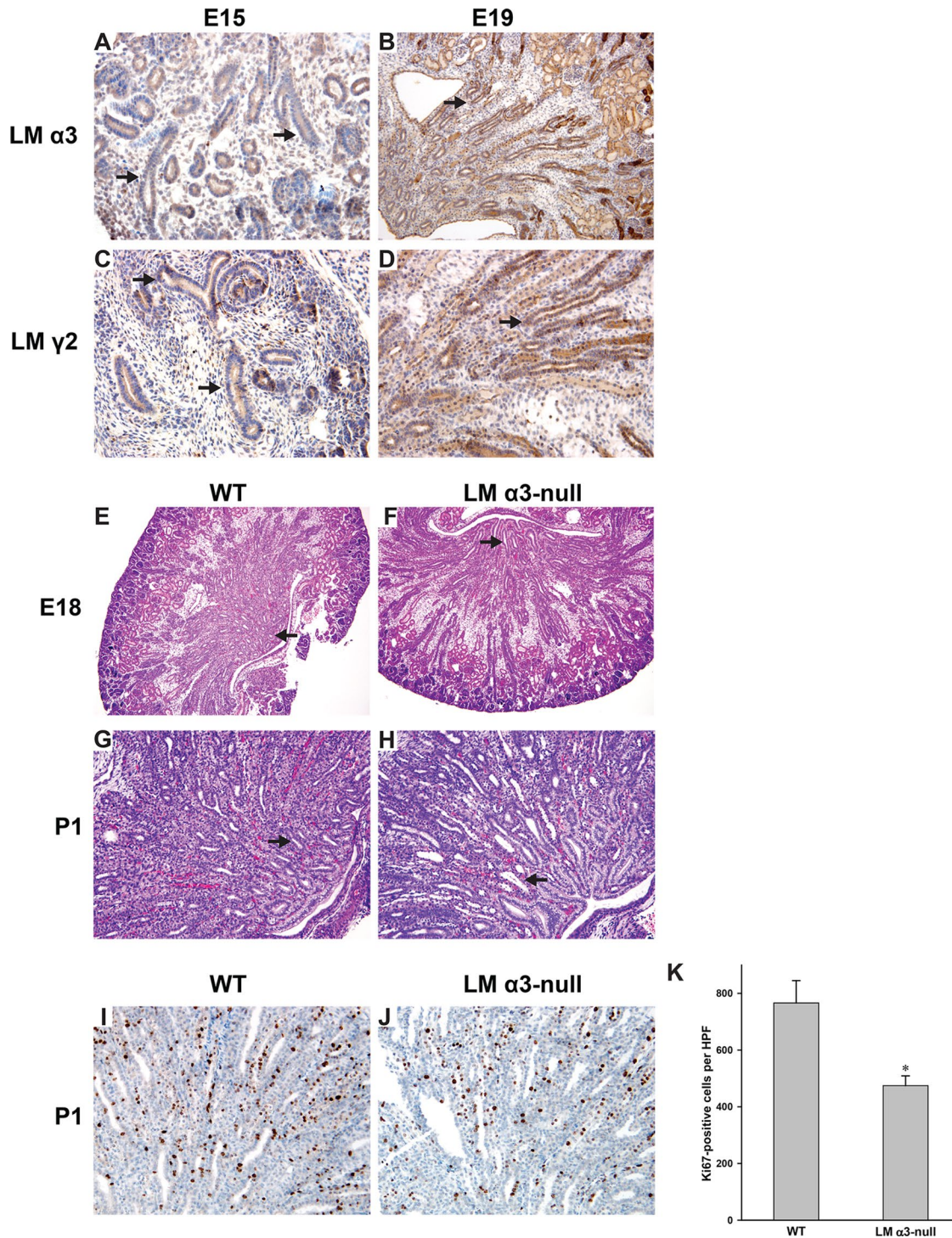


FIGURE 1: The LM $\alpha 3$ chain is required for normal UB development. (A–D) Embryonic mouse kidneys (E15, E19) stained with antibody against the LM $\alpha 3$ or LM $\gamma 2$ chain. The UB is designated by the arrows (100 \times magnification). (E–H) H&E-stained kidneys of WT and LM $\alpha 3$ -null mice at E18 and postnatal day 1 (P1). Magnification is 40 \times (E and F) and 100 \times (G and H). The arrows indicate the hypoplastic dysplastic papilla with dilated CDs present in the LM $\alpha 3$ -null relative to WT mice. (I and J) Embryonic mouse kidneys (E19) stained with Ki67 antibody (100 \times magnification). (K) Bar graph of the average numbers of Ki67-positive tubular cells per HPF 100 \times magnification field of inner medullary CDs (6 HPF, 3 mice of each genotype) with SEM, *, $p < 0.05$ between WT and LM $\alpha 3$ -null.

(Figure 2, C–H). Hypoplastic/dysplastic papillae persisted into adulthood of the *Hoxb7Cre;Itg $\alpha 3^{flox/flox}$* mice (Figure 2, I–L).

As deleting the $\beta 1$ integrin subunit in the UB resulted in markedly decreased activating phosphorylation of focal adhesion kinase (FAK), Akt, ERK1/2, and p38 MAPK (Zhang *et al.*, 2009), we

examined whether similar abnormalities occurred in the developing collecting system of *Hoxb7Cre;Itg $\alpha 3^{flox/flox}$* mice. As for the $\beta 1$ -null mice, we noted a decrease in Akt and p38 phosphorylation in the UB of *Hoxb7Cre;Itg $\alpha 3^{flox/flox}$* mice; however, FAK (unpublished data) and ERK1/2 (Figure 2M) activation were

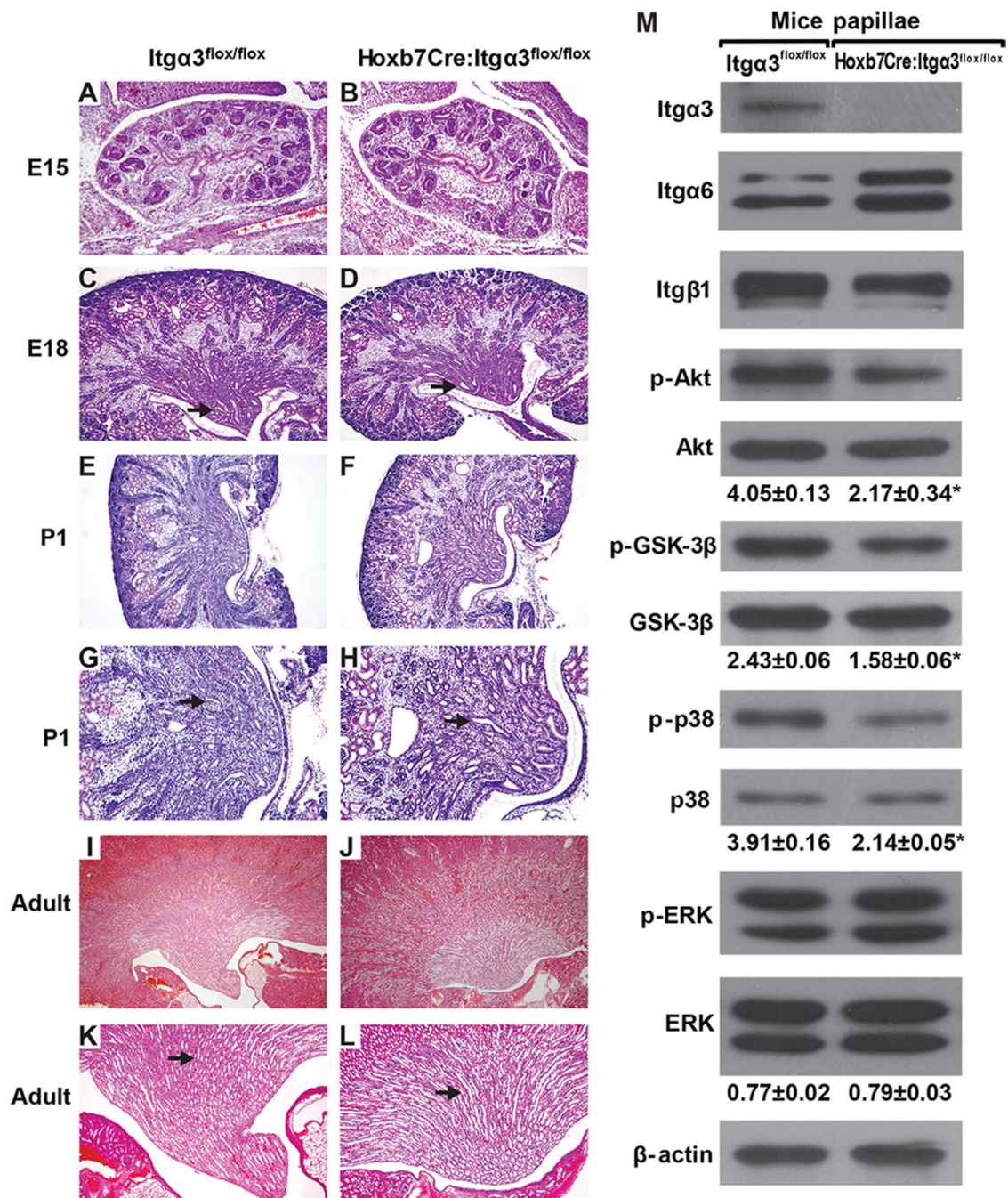


FIGURE 2: Hoxb7Cre:Itga3^{flox/flox} mice have defective UB development and decreased activation of Akt, GSK-3β, and p38 MAPK. (A–L) H&E stained kidneys of WT mice (Itga3^{flox/flox}) and mice lacking integrin α3 in the UB (Hoxb7:Itga3^{flox/flox}) at various stages of development. Magnification is 40× (A–F, I, and J) and 100× (G, H, K, and L). Note the mild branching defect from E15 onward and the hypoplastic papilla, which is characterized by fewer but dilated CDs in the Hoxb7:Itga3^{flox/flox} mice from E18 onward (arrows). (M) Lysates of papillae (20 μg total protein/lane) from 3-d-old Itga3^{flox/flox} and Hoxb7:Itga3^{flox/flox} mice were analyzed by Western blotting for levels of integrin subunits α3, α6, and β1; phospho-Akt^{Ser473}, phospho-GSK-3β, phospho-p38, and phospho-ERK1/2. Bands of phosphorylated and total proteins as well as β-actin (loading control) were measured by densitometry. The amount of phosphorylated proteins was normalized to total protein and β-actin levels and presented as mean ± SEM from at least three animals; *, *p* < 0.05 between Hoxb7:Itga3^{flox/flox} and Itga3^{flox/flox} samples.

unaffected. Consistent with diminished Akt activation, there was decreased Akt-dependent phosphorylation of glycogen synthase kinase 3 beta (GSK-3β) at Ser9 (Figure 2M). These data suggest that integrin α3 subunit regulates a limited number of integrin β1-dependent signaling pathways in the developing kidney collecting system, specifically the Akt and p38 MAPK pathways. Of

note, deletion of α3 integrin subunit resulted in decreased expression of β1 and increased expression of α6 integrin subunits (Figure 2M). These data suggest that α3 is the major integrin subunit that interacts with the β1 subunit in the renal papilla and that there is compensatory expression of the integrin α6 subunit upon its deletion.

Integrin $\alpha 3$ -null CD cells have severe adhesion, migration, proliferation, and signaling defects on LM-332

To study the mechanisms whereby LM/integrin $\alpha 3\beta 1$ interactions regulate collecting system development, we isolated CD cells from $\text{Itg}\alpha 3^{\text{flox/flox}}$ mice ($\text{Itg}\alpha 3^{\text{ff}}$) and deleted the integrin $\alpha 3$ subunit in vitro by infecting the cells with adeno-cre ($\text{Itg}\alpha 3^{-/-}$). As seen in the renal papilla, integrin $\alpha 3$ deletion led to increased integrin $\alpha 6$ and decreased integrin $\beta 1$ expression (Figure 3, A and B). Interestingly, the increased $\alpha 6$ integrin subunit was associated with $\beta 1$ and the level of integrin $\alpha 6\beta 4$ was unchanged (Figure 3C). There was no change in expression of $\alpha 1$, $\alpha 2$, $\alpha 5$, or αv integrin subunits (unpublished data), suggesting that the expression levels of the collagen- and arginine-glycine-aspartic acid (RGD)-binding integrins were unaffected. Thus, as in the renal papilla, $\alpha 3$ appears to be the principal integrin subunit that interacts with the $\beta 1$ subunit in CD cells, and there is compensatory expression of the integrin $\alpha 6$ subunit upon its deletion.

On the basis of our in vivo studies and those of others demonstrating that $\text{Hoxb7Cre};\text{Itg}\alpha 3^{\text{flox/flox}}$ mice have similar phenotypes to LM $\alpha 5$ - and $\alpha 3$ -null mice (Miner and Li, 2000; Liu et al., 2009; Figure 1), we defined whether integrin $\alpha 3\beta 1$ controls CD cell adhesion, migration, and proliferation by interacting with LM-511 and/or LM-332. Severe defects in all these cell functions were detected for $\text{Itg}\alpha 3^{-/-}$ CD cells plated on LM-332. In contrast, the defects on LM-511, while significant, were not as severe (Figure 3, D–G), suggesting that LM-332 is a preferred substrate for integrin $\alpha 3\beta 1$. To confirm the specific role of integrin $\alpha 3\beta 1$ and the $\alpha 6$ -containing integrins on CD cell adhesion to LM-332 and LM-511, we performed adhesion assays in the presence of a blocking anti- $\text{Itg}\alpha 6$ antibody (Figure 3H). Blocking $\alpha 6$ -containing integrins did not affect adhesion of $\text{Itg}\alpha 3^{\text{ff}}$ CD cells to LM-332 but decreased adhesion of these cells to LM-511. Adhesion of $\text{Itg}\alpha 3^{-/-}$ CD cells to both LMs was decreased by the addition of anti- $\text{Itg}\alpha 6$ antibody (Figure 3H). Thus $\alpha 6$ -containing integrins play a role in CD cell binding to LM-511 in the presence and absence of integrin $\alpha 3\beta 1$; however, they only affect CD cell adhesion to LM-332 in the absence of integrin $\alpha 3\beta 1$. LM-332 and LM-511 were verified as specific substrates for integrin $\alpha 3\beta 1$, as no differences between $\text{Itg}\alpha 3^{\text{ff}}$ and $\text{Itg}\alpha 3^{-/-}$ cells were found when these assays were performed on collagen I, fibronectin, vitronectin, or LM-111 (Supplemental Figure 2).

Integrin $\alpha 3\beta 1$ -dependent adhesion to LM-332 and LM-511 activates Akt and p38 signaling pathways in CD cells

As our in vivo data demonstrated decreased Akt and p38 activation in the $\text{Hoxb7Cre};\text{Itg}\alpha 3^{\text{flox/flox}}$ mice (Figure 2M), we performed in vitro replating assays to define whether the defects observed in cell function were mediated by abnormalities in integrin $\alpha 3\beta 1$ -LM-dependent signaling. $\text{Itg}\alpha 3^{-/-}$ CD cells failed to significantly increase Akt phosphorylation when plated on LM-332 or LM-511 (Figure 4A). A similar defect in Akt-dependent phosphorylation of GSK-3 β was also seen when $\text{Itg}\alpha 3^{-/-}$ CD cells were plated on LM-332 or LM-511 (Figure 4A). It is important to note that the basal levels of Akt and Akt-dependent GSK-3 β phosphorylation were significantly higher in $\text{Itg}\alpha 3^{-/-}$ than in $\text{Itg}\alpha 3^{\text{ff}}$ CD cells (an approximately twofold difference; Figure 4A). There were also less marked but significant abnormalities in p38 signaling characterized by less-sustained activation in $\text{Itg}\alpha 3^{-/-}$ CD cells plated on either LM-332 or LM-511 compared with $\text{Itg}\alpha 3^{\text{ff}}$ CD cells (Figure 4A). No difference in ERK1/2 activation was seen between the two CD cell populations. These results suggest that integrin $\alpha 3\beta 1$ mediates LM-dependent activation of both Akt and p38 pathways; however, the effects on Akt are more profound. As with cell adhesion, migration, and proliferation (Figure 3, D–G), integrin $\alpha 3\beta 1$ induced

these signaling pathways more strongly when it interacted with LM-332 than with LM-511.

The role of p38 MAPK on integrin $\alpha 3\beta 1$ -dependent CD cell adhesion and migration on LM-332 was investigated by inhibiting its activity with SB203580 in $\text{Itg}\alpha 3^{\text{ff}}$ CD cells. Inhibition of p38 MAPK, which was verified by decreased phosphorylation of MAPK-APK2, a specific downstream target of p38 MAPK (Figure 4B), resulted in a severe adhesion and migration defect (Figure 4, C and D). These data confirmed a role of p38 MAPK for integrin $\alpha 3\beta 1$ -dependent adhesion to and migration on LM-332.

Akt signaling pathway is critical for integrin $\alpha 3\beta 1$ -dependent CD cell adhesion and migration on LM-332

Because deleting the integrin $\alpha 3$ subunit caused increased basal Akt signaling and the inability to activate this pathway further, we defined the functional significance of Akt activation on integrin $\alpha 3\beta 1$ -dependent CD cell adhesion and migration on the preferred integrin $\alpha 3\beta 1$ substrate LM-332. This was done by inhibiting its activity using two distinct Akt small interfering RNAs (siRNAs) or Akt inhibitor IV in $\text{Itg}\alpha 3^{\text{ff}}$ CD cells (Figure 5, A and B) and then defining the ability of these cells to adhere and migrate (Figure 5, C and D). These treatments resulted in a significant decrease in cell adhesion to and migration on LM-332 (Figure 5, C and D). We confirmed that adhesion of CD cells to LM-332 was dependent on Akt signaling by restoring normal basal cell adhesion by transducing the cells with an adenovirus expressing constitutively active myristoylated Akt (Figure 5E). Analysis of signaling pathway activation revealed that Akt inhibitor IV treatment prevented phosphorylation of Akt and its downstream target GSK-3 β (Figure 5B).

Integrin $\alpha 3\beta 1$ -dependent CD cell adhesion to and migration on LM-332 requires PI3K-independent Akt activation

A key regulator of Akt activity is PI3K, which phosphorylates PIP₂ to PIP₃ to create membrane sites for the Akt pleckstrin homology domain binding that allows for Akt recruitment to the plasma membrane, where it is activated (Cantley, 2002). To determine whether PI3K activity plays a role in integrin $\alpha 3\beta 1$ -dependent adhesion to and migration on LM-332, we inhibited PI3K activity by infecting the $\text{Itg}\alpha 3^{\text{ff}}$ cells with adenovirus carrying a catalytic subunit deletion PI3K mutant, ad-delta p85 (Figure 6A). Surprisingly, both cell adhesion and migration were not affected by this form of PI3K inhibition (Figure 6, B and C). Similar results were obtained with the selective PI3K inhibitor LY294002 (Figure 6, B and C). Signaling pathway analysis revealed that LY294002 prevented Akt phosphorylation at the PI3K/PDK1-dependent Thr308 site (Figure 6D); however, phosphorylation of Ser473, which is performed by mTORC2 and serves as an indication of full Akt activation (Cantley, 2002; Guertin and Sabatini, 2007), was not affected (Figure 6D). Taken together, these data demonstrate that, in CD cells, Akt activity required for integrin $\alpha 3\beta 1$ -dependent adhesion to and migration on LM-332 is PI3K independent.

We next defined the mechanisms whereby integrin $\alpha 3\beta 1$ regulates PI3K-independent activation of Akt in response to adhesion to LM by measuring the PIP₃ levels in $\text{Itg}\alpha 3^{\text{ff}}$ and $\text{Itg}\alpha 3^{-/-}$ CD cells upon plating on LM-332. Basal levels of PIP₃ in $\text{Itg}\alpha 3^{-/-}$ CD cells were significantly higher than those detected in $\text{Itg}\alpha 3^{\text{ff}}$ CD cells (Figure 6E). However, following plating on LM-332, $\text{Itg}\alpha 3^{\text{ff}}$ CD cells showed a dramatic increase in PIP₃ levels (~1000-fold). In contrast, decreased levels of PIP₃ were noted in $\text{Itg}\alpha 3^{-/-}$ CD cells (Figure 6E).

In addition to PI3K, the amount of PIP₃ in cellular membranes is regulated by PTEN (Cantley, 2002; Song et al., 2012). We therefore determined whether PTEN is responsible for the observed differences in PIP₃ levels. Indeed, the higher basal amount of PIP₃ in

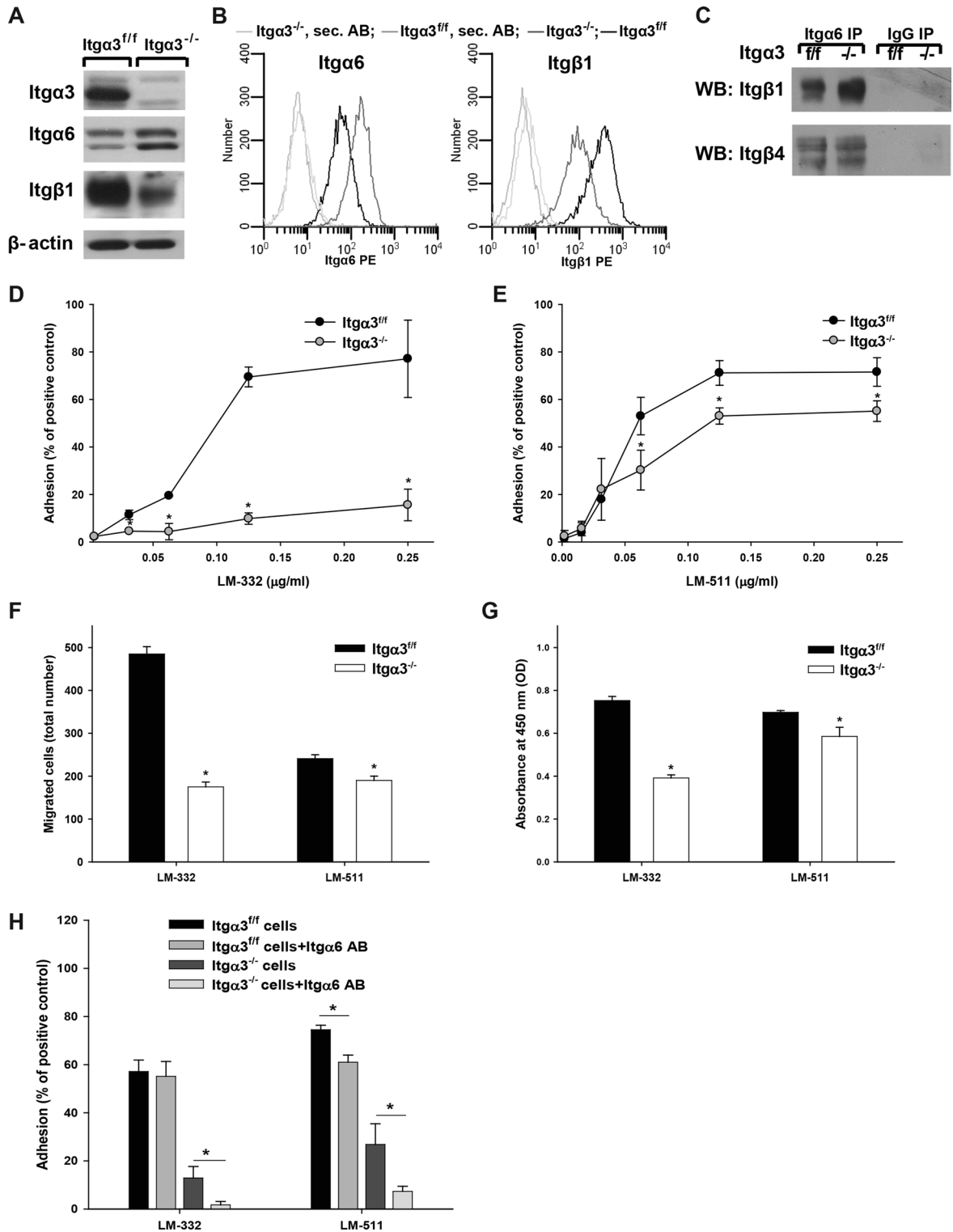


FIGURE 3: Integrin $\alpha 3\beta 1$ promotes CD cell adhesion, migration, and proliferation on LM-332 and LM-511. (A) Lysates from $Itga3^{-/-}$ and $Itga3^{f/f}$ CD cells (20 μ g total protein/lane) were immunoblotted for integrin $\beta 1$, $\alpha 3$, and $\alpha 6$ subunits. β -actin served as a loading control. (B) Surface expression of integrin $\beta 1$, $\alpha 3$, and $\alpha 6$ subunits was determined on $Itga3^{-/-}$ and $Itga3^{f/f}$ CD cells by flow cytometry using R-phycoerythrin (PE). (C) Lysates from $Itga3^{-/-}$ and $Itga3^{f/f}$ CD cells (100 μ g total protein) were immunoprecipitated with anti- $Itga6$ antibody or normal rabbit IgG and immunoblotted for integrin subunits $\beta 1$ and $\beta 4$. Adhesion (D and E), migration (F), and proliferation (G) of $Itga3^{f/f}$ and $Itga3^{-/-}$ CD cells on LM-332 and LM-511 were evaluated as described in *Materials and Methods*. Mean measurements \pm SEM of four to six independent experiments are shown; *, $p \leq 0.05$ between $Itga3^{f/f}$ and $Itga3^{-/-}$ CD cells. (H) $Itga3^{f/f}$ and $Itga3^{-/-}$ CD cells were treated with blocking anti- $Itga6$ antibody and plated on LM-332. Adhesion was evaluated as described in *Materials and Methods*. Mean measurements \pm SEM of three independent experiments are shown; *, $p \leq 0.05$ between CD cells and CD cells treated with blocking anti- $Itga6$ antibody.

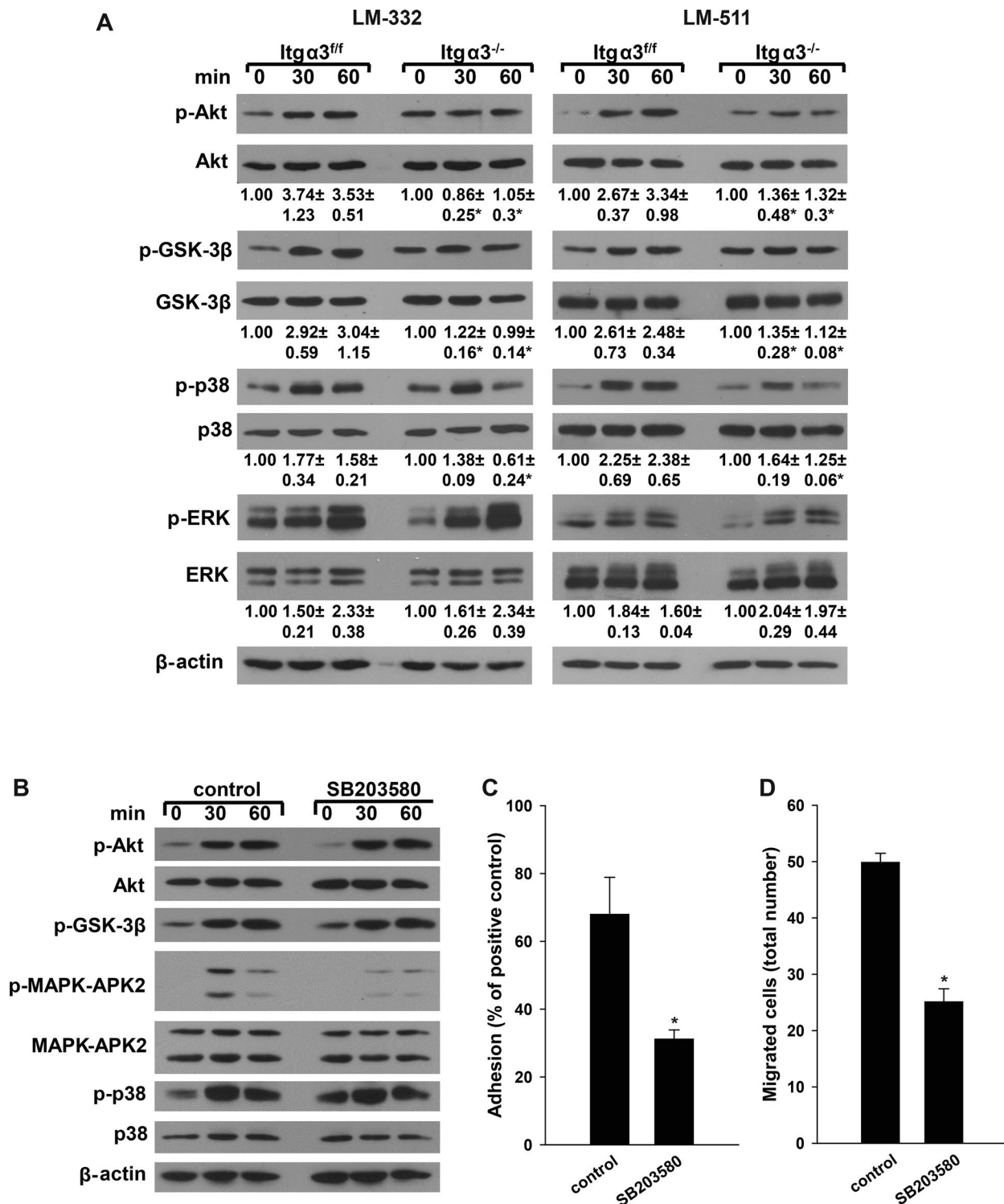


FIGURE 4: Integrin $\alpha 3\beta 1$ -dependent adhesion induces activation of Akt and p38 pathways. (A) Itg $\alpha 3^{+/f}$ and Itg $\alpha 3^{-/-}$ CD cells were plated in serum-free medium on LM-332 or LM-511 (both at 1 μ g/ml). Cells were lysed at 30 and 60 min after plating, and lysates were analyzed by Western blotting for levels of phosphorylated Akt^{Ser473}, GSK-3 β , p38, and ERK1/2 (20 μ g total protein/lane). Levels of phosphorylated proteins were measured by densitometry, normalized to total protein and β -actin levels, and expressed as fold change relative to cells left in suspension, "0" time point. Values are the mean \pm SEM of three independent experiments; *, $p \leq 0.05$ between Itg $\alpha 3^{+/f}$ and Itg $\alpha 3^{-/-}$ CD cells. (B–D) Itg $\alpha 3^{+/f}$ CD cells were treated with dimethyl sulfoxide (DMSO; control) or the p38 inhibitor SB203580 (10 μ M) for 1 h, after which the cells were trypsinized; resuspended in serum-free medium; and subjected to replating (B), adhesion (C), or migration (D) assays on LM-332 (1 μ g/ml). (B) Cell signaling was evaluated by immunoblotting cell lysates for phosphorylated Akt^{Ser473}, GSK-3 β , p38, and MAPK-APK2 (20 μ g total protein/lane). β -actin served as a loading control. Adhesion (C) and migration (D) were evaluated as described in *Materials and Methods*. Mean measurements \pm SEM of three independent experiments are shown; *, $p \leq 0.05$ between Itg $\alpha 3^{+/f}$ treated with DMSO and SB203580.

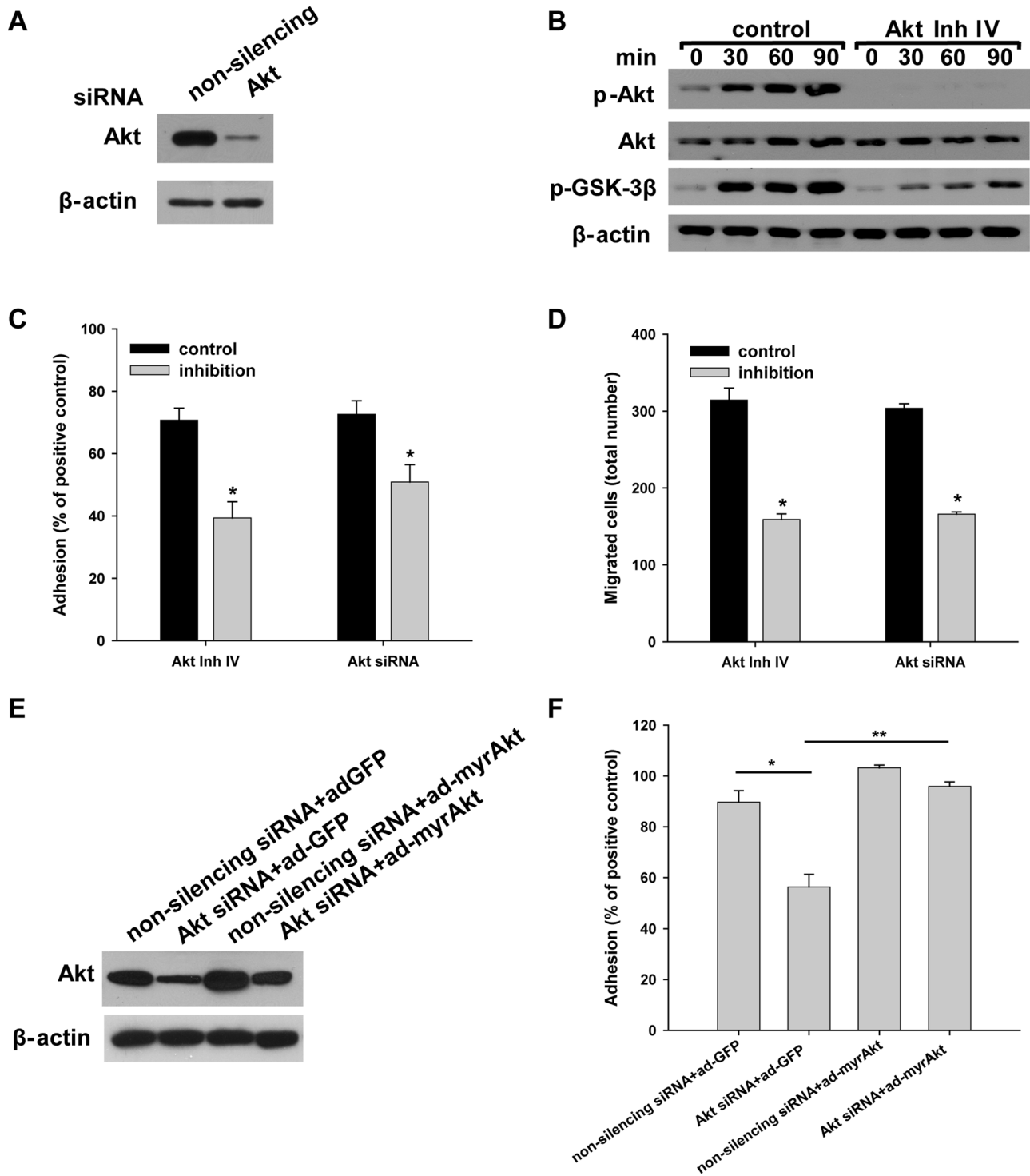


FIGURE 5: Integrin $\alpha 3\beta 1$ -dependent adhesion and migration on LM-332 are regulated by Akt activation. *Itg $\alpha 3^{fl/fl}$* CD cells were transfected with nonsilencing or Akt siRNA (100 nM for 48 h) (A and C–F) or treated with the Akt inhibitor IV (5 μ M for 1 h) or DMSO (control) (B–D). The effect of the siRNA on AKT expression is shown by immunoblotting cell lysates for total Akt, with β -actin serving as a loading control (A). (B–D) Control cells or cells treated with Akt inhibitor IV were subjected to replating, after which cell lysates were immunoblotted for phosphorylated Akt^{Ser473} and GSK-3 β and total Akt (20 μ g total protein/lane), with β -actin serving as a loading control (B). Treated and untreated cells were evaluated for adhesion (C) or migration (D) on LM-332 (1 μ g/ml) and evaluated as described in *Materials and Methods*. Mean measurements \pm SEM of four to six independent experiments are shown; *, $p \leq 0.05$ between control *Itg $\alpha 3^{fl/fl}$* cells and *Itg $\alpha 3^{fl/fl}$* cells with inhibitors. (E and F) *Itg $\alpha 3^{fl/fl}$* CD cells were transfected with either nonsilencing or Akt siRNA, with control (ad-GFP) or myristilated Akt (100 plaque-forming units/cell for 24 h) (myrAkt) (E) and subjected to an adhesion assay as described in C (F). Mean measurements \pm SEM of four to six independent experiments are shown; *, $p \leq 0.05$ between control *Itg $\alpha 3^{fl/fl}$* cells and *Itg $\alpha 3^{fl/fl}$* cells transfected with Akt siRNA; *, $p \leq 0.05$ between *Itg $\alpha 3^{fl/fl}$* cells with Akt siRNA and *Itg $\alpha 3^{fl/fl}$* cells with Akt siRNA and myristilated Akt.

Itg $\alpha 3^{-/-}$ CD cells (Figure 6E) correlated with lower basal PTEN levels (Figure 6F) and higher basal Akt activity (Figure 4A). Following plating on LM-332, PTEN levels decreased in Itg $\alpha 3^{+/f}$ CD cells but increased in Itg $\alpha 3^{-/-}$ CD cells (Figure 6F). By contrast, PIP $_3$ levels and Akt activity increased in Itg $\alpha 3^{+/f}$ CD cells, but decreased in Itg $\alpha 3^{-/-}$ CD cells (Figures 6E and 4A). These data suggest that integrin $\alpha 3\beta 1$ regulates PIP $_3$ levels and, in turn, Akt activation by regulating PTEN levels.

There are two signaling events in the canonical pathway of Akt activation that precede and follow the membrane-anchoring step: Src-dependent Akt phosphorylation preconditions Akt for membrane binding, and PDK1-mediated phosphorylation activates membrane-bound Akt (Cantley, 2002; Jiang and Qiu, 2003; Bayascas, 2008). No differences in Src or PDK1 activation were noted between Itg $\alpha 3^{+/f}$ and Itg $\alpha 3^{-/-}$ CD cells plated on LM-332 (Figure 6F), suggesting that these kinases were not responsible for the differences in Akt activation between the two cell populations. As Src and PDK1 activities are regulated by PI3K, these data further confirm that integrin $\alpha 3\beta 1$ regulates Akt activity via a PI3K-independent mechanism(s).

Integrin $\alpha 3\beta 1$ -dependent K63-linked polyubiquitination of Akt is mediated by TRAF6

K63-linked polyubiquitination of Akt is also an essential step in Akt activation (Yang *et al.*, 2009, 2010). While the mechanism is unclear, it has been postulated that K63-linked polyubiquitination increases Akt binding to PI(3,4,5)P $_3$ on the membrane or creates docking sites for Akt to interact with other signaling proteins (Wang *et al.*, 2012). We therefore checked for differences in K63-linked polyubiquitination between Itg $\alpha 3^{+/f}$ and Itg $\alpha 3^{-/-}$ CD cells plated on LM-332 by immunoblotting for K63-linked polyubiquitination of Akt immunoprecipitates (Figure 7A). K63-linked polyubiquitination of Akt increased over time when Itg $\alpha 3^{+/f}$ CD cells were plated on LM-332, while no significant change was noted in the Itg $\alpha 3^{-/-}$ CD cells (Figure 7A). Of note, the basal level of Akt K63-linked polyubiquitination was significantly higher in Itg $\alpha 3^{-/-}$ than in Itg $\alpha 3^{+/f}$ CD cells (an approximately twofold difference; Figure 7A). To verify the specificity of the Akt K63-linked polyubiquitination, we measured Akt K48-linked polyubiquitination in Itg $\alpha 3^{+/f}$ and Itg $\alpha 3^{-/-}$ CD cells and found that this was unaffected by adhesion to LM-332 (Figure 7B). Thus integrin $\alpha 3\beta 1$ -dependent CD cell adhesion to LM specifically increases K63-linked polyubiquitination of Akt.

TRAF6 was recently identified as a unique E3 ligase for Akt that is responsible for K63-linked Akt polyubiquitination, which facilitates Akt membrane recruitment and subsequent Akt phosphorylation and activation (Yang *et al.*, 2009; Wang *et al.*, 2012). We therefore determined whether the ubiquitination activity of TRAF6 was altered by integrin $\alpha 3\beta 1$ -dependent adhesion to LM-332 by measuring TRAF6 K63-linked autopolyubiquitination (Lamothe *et al.*, 2007). This was indeed the case, as K63-linked polyubiquitination of TRAF6 increased significantly when Itg $\alpha 3^{+/f}$ CD cells adhered to LM-332, while no increase above basal levels was seen in Itg $\alpha 3^{-/-}$ CD cells (Figure 7C). Of note, the basal level of TRAF6 K63-linked polyubiquitination was significantly higher in Itg $\alpha 3^{-/-}$ than in Itg $\alpha 3^{+/f}$ CD cells (an approximately twofold difference; Figure 7C), which would explain the increased basal Akt ubiquitination and activation observed in Itg $\alpha 3^{-/-}$ CD cells (see Figure 4A for details).

The functional significance of TRAF6 activity for integrin $\alpha 3\beta 1$ -dependent Akt activation was then defined by down-regulating its expression in Itg $\alpha 3^{+/f}$ CD cells using an siRNA approach (Figure 7D). Reduced TRAF6 expression resulted in a severe defect in Akt phosphorylation (Figure 7D) and decreased K63-linked polyubiquitination of Akt when Itg $\alpha 3^{+/f}$ CD cells were plated on LM-332 (Figure 7E).

We next defined the functional effects of down-regulating TRAF6 on integrin $\alpha 3\beta 1$ -dependent cell adhesion to LM-332 and found that decreased TRAF6 expression significantly decreased Itg $\alpha 3^{+/f}$ CD cells adhesion to this substrate (Figure 7F). As this decreased adhesion was similar to that induced by the Akt inhibitor IV (Figure 7F), we postulated that TRAF6 might regulate cell adhesion by altering the activation state of Akt. This possibility was confirmed by the fact that introduction of a constitutively active Akt (ad-myrAkt) restored the adhesion defects caused by TRAF6 down-regulation (Figure 7F).

TRAF6 deficiency causes renal papilla dysplasia/hypoplasia and defects in Akt signaling

Our *in vitro* data suggested that integrin $\alpha 3\beta 1$ regulates Akt activation by altering TRAF6 function in CD cells. We therefore investigated whether TRAF6-dependent activation of Akt regulates kidney collecting system development *in vivo* by analyzing the phenotype of kidneys from TRAF6-deficient (KO) mice. Previous investigation of these animals has demonstrated that TRAF6 is essential for normal bone formation (Lomaga *et al.*, 1999), establishment of the immune system and inflammatory response (Lomaga *et al.*, 1999; Naito *et al.*, 1999), development of the central neuron system (Lomaga *et al.*, 2000) and epidermal appendices (Naito *et al.*, 1999). The kidneys of TRAF6 KO newborn mice were noticeably smaller than wild-type (WT) animals (Figure 8, A and B). When we examined the kidneys of TRAF6 KO newborn mice in detail, we noted a slight branching morphogenesis defect in the renal collecting system and a mildly dysplastic papilla (Figure 8, C and D) resembling the defects observed in the Hoxb7Cre;Itg $\alpha 3^{flox/flox}$ (Figure 2, E–H) and the constitutive Itg $\alpha 3$ -null mice (Kreidberg *et al.*, 1996). As deleting the $\alpha 3$ integrin subunit in the UB resulted in markedly decreased activation of Akt signaling (Figure 2M), we examined whether similar abnormalities occurred in the developing collecting system of TRAF6 KO mice. As in Hoxb7Cre;Itg $\alpha 3^{flox/flox}$ mice, we noted a decrease in Akt activation of phosphorylation in the collecting system of the TRAF6 KO mice (Figure 8E). Consistent with decreased Akt activation, there was decreased Akt-dependent phosphorylation of GSK-3 β at Ser9 (Figure 8E). These data suggest that TRAF6 regulates activity of the Akt signaling pathway in the developing kidney collecting system.

TRAF6 forms a complex with $\alpha 3\beta 1$ integrin and Akt

Finally, we defined how $\alpha 3\beta 1$ integrin and TRAF6 interact with each other to mediate K63-linked polyubiquitination of Akt. This question was addressed by immunoprecipitating integrin $\alpha 3$ or $\beta 1$ subunits from Itg $\alpha 3^{+/f}$ and Itg $\alpha 3^{-/-}$ CD cells grown on uncoated cell culture plates. The immunoprecipitates were immunoblotted for integrin $\beta 1$ and $\alpha 3$ subunits or TRAF6 (Figure 9, A and B). The $\beta 1$ integrin subunit was present in $\alpha 3$ immunoprecipitates from Itg $\alpha 3^{+/f}$ but not Itg $\alpha 3^{-/-}$ CD cells (Figure 9A). TRAF6 was not detected in Itg $\alpha 3$ immunoprecipitates from Itg $\alpha 3^{+/f}$ or Itg $\alpha 3^{-/-}$ CD cells (Figure 9A). We believe this is a result of very low immunoprecipitation efficiency. In this regard, Figure 9A shows that ~5% of integrin $\alpha 3$ immunoprecipitates with the anti-Itg $\alpha 3$ antibody, which allows us to detect bound integrin $\beta 1$. However, since TRAF6 likely binds inferiorly to integrin $\alpha 3\beta 1$ via the cytoplasmic tail of integrin $\beta 1$, it does not allow for TRAF6 detection. As expected, there were fewer $\beta 1$ and no $\alpha 3$ integrin subunits in the Itg $\beta 1$ immunoprecipitates from Itg $\alpha 3^{-/-}$ compared with Itg $\alpha 3^{+/f}$ CD cells (Figure 9B). TRAF6 was immunoprecipitated from lysates of Itg $\alpha 3^{+/f}$ but not Itg $\alpha 3^{-/-}$ CD cells (Figure 9B). We next defined the integrin subunit to which TRAF6 binds by performing affinity chromatography of CD cell lysates with His-tagged $\beta 1$, $\alpha 3$, or $\alpha 5$ (used as negative control) transmembrane and

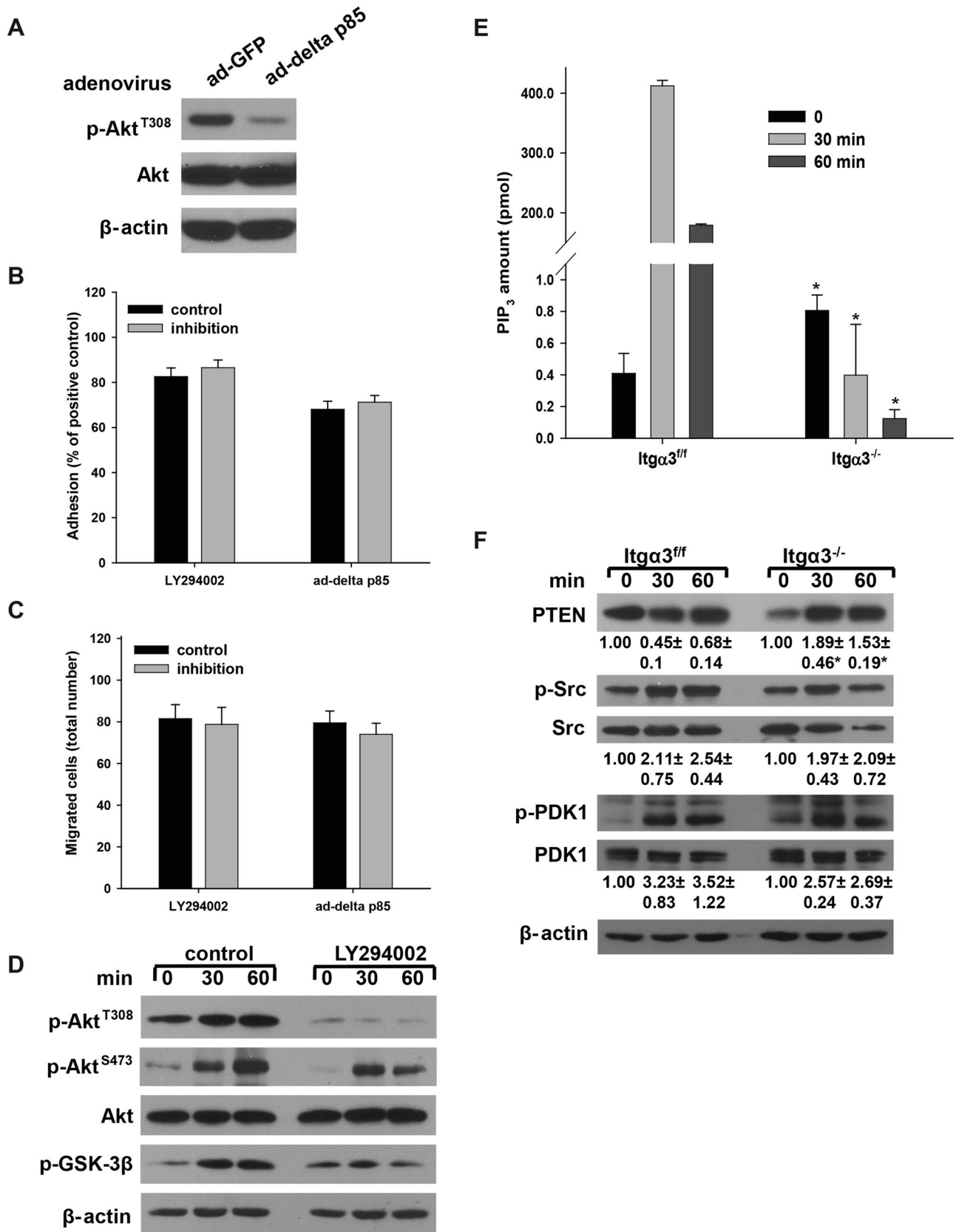


FIGURE 6: Integrin $\alpha 3\beta 1$ -dependent CD cell adhesion to and migration on LM-332 requires PI3K-independent Akt activation. (A–D) $Itg\alpha 3^{ff}$ CD cells were infected with ad-GFP or ad-delta p85 (100 plaque-forming units/cell for 24 h) (A); or treated with DMSO (control) or the PI3K inhibitor LY294002 (25 μ M for 1 h). Cells were subjected to adhesion (B), migration (C), or the replating assay on LM-332 (1 μ g/ml) for evaluation of phospho-Akt^{Thr308}, phospho-Akt^{Ser473}, and phospho-GSK-3 β . β -actin served as a loading control. Western blot of cellular lysates shows that infection with ad-delta

cytoplasmic tail peptides. Interestingly, TRAF6 and kindlin 2 (which is known to bind specifically to $\beta 1$ integrin) bound to integrin $\beta 1$ but not to $\alpha 3$ or $\alpha 5$ cytoplasmic tails (Figure 9C). Together these data suggest that TRAF6 binds to the cytoplasmic tail of the $\beta 1$ integrin subunit, and this interaction requires the presence of the $\alpha 3$ integrin subunit in cells expressing intact $\beta 1$ integrin.

We next defined whether TRAF6 associates with Akt and whether this association is regulated by integrin $\alpha 3\beta 1$ interactions with LM. When CD cells were plated on LM-332, more Akt coimmunoprecipitated with TRAF6 in a time-dependent manner in $\text{Itg}\alpha 3^{\text{fl/fl}}$ compared with $\text{Itg}\alpha 3^{-/-}$ cells. These data suggest that TRAF6 and Akt form a complex following integrin $\alpha 3\beta 1$ -dependent adhesion (Figure 9D).

DISCUSSION

Integrin $\alpha 3\beta 1$ plays an important role in UB development in vivo due to its interactions with $\alpha 5$ -containing LMs, and in vitro studies suggested these effects are mediated by its ability to regulate PI3K/Akt-dependent Wnt signaling (Liu et al., 2009). In this study, we show that $\alpha 3$ -containing LMs, in addition to the $\alpha 5$ LMs, play a crucial part in UB development and that integrin $\alpha 3\beta 1$ regulates both Akt and p38 activation in the UB in vivo. We also demonstrate that LM-332 is the preferred ligand for mediating integrin $\alpha 3\beta 1$ -dependent CD cell functions and signaling. Finally, and most importantly, we establish that the integrin $\beta 1$ cytoplasmic tail interacts with TRAF6, which is an E3 ligase for K63-linked polyubiquitination, and this interaction regulates integrin $\alpha 3\beta 1$ -dependent Akt activation and cell functions. Thus these studies define a novel functionally important LM-integrin $\alpha 3\beta 1$ interaction in UB development and identify K63-linked polyubiquitination as a critical new mechanism whereby integrins modulate cell signaling.

We previously demonstrated that LM-332 is expressed during initial UB formation and that it plays a significant role in in vitro cell and organ culture models of UB development (Zent et al., 2001). Consistent with these findings, we demonstrate in this study that the $\alpha 3$ and $\gamma 2$ LM chains are expressed during UB development and that deleting the $\alpha 3$ LM chain results in a severe renal development abnormality in outbred mice (with 40% of mice not developing one kidney) and a mild to moderate branching defect in pure C57/Bl6 mice. Interestingly, no phenotype was observed in the developing UB of the LM $\gamma 2$ -null mice (unpublished data), suggesting functional redundancy of the $\alpha 3$ LMs in UB development. The mild to moderate phenotype in LM $\alpha 3$ -null mice is similar to that seen in LM $\alpha 5$ -null mice (Liu et al., 2009) and much less severe than when the LM $\gamma 1$ chain was selectively deleted in the developing UB (Yang et al., 2011). Our finding that LM $\alpha 3$ plays a role in UB development might explain the less severe than expected phenotype in the LM $\gamma 1$ -null mice, as LM-332 could be compensating for the LM $\gamma 1$ deletion (Yang et al., 2011).

When we deleted the integrin $\alpha 3$ subunit in the UB, we observed a mild to moderate branching morphogenesis defect at E15 that persisted into adulthood. These results differ slightly from previous

observations that the UB of constitutive integrin $\alpha 3$ -null kidneys at E15 was indistinguishable from WT mice and that a difference was seen only at E18, when the null kidneys demonstrated a failure of papillary outgrowth (Kreidberg et al., 1996; Liu et al., 2009). These discrepancies could be due to differences in mouse backgrounds or because the Hoxb7Cre and integrin $\alpha 3^{\text{lox/lox}}$ mice were generated using different strategies.

Deleting the $\alpha 3$ integrin subunit in the UB in vivo and in CD cells resulted in decreased expression of the $\beta 1$ and increased expression of the $\alpha 6$ integrin subunits, suggesting that $\alpha 3$ is the major integrin subunit that interacts with the $\beta 1$ subunit in the renal papilla and there is compensatory expression of the integrin $\alpha 6$ subunit upon its deletion. The increased $\alpha 6$ expression might explain the mild phenotypic defects observed when the integrin $\alpha 3$ subunit is deleted from the UB (Kreidberg et al., 1996; Liu et al., 2009) and why it is significantly less severe than that seen when kidneys or isolated UBs are grown in the presence of $\alpha 3$ -blocking antibodies (Zent et al., 2001). This possibility is further supported by our in vitro data showing that $\alpha 6\beta 1$ integrin contributes to increased CD cell binding to LM-332 and LM-511, especially in the absence of integrin $\alpha 3\beta 1$ expression. Although it is not proven, we speculate that the $\alpha 6\beta 1$ compensation occurs through a distinct TRAF6-independent mechanism.

We show that LM-332 is the preferred LM for CD cell adhesion, migration, proliferation, and adhesion-dependent cell signaling. These data are consistent with findings demonstrating a role for LM-332 in regulating proliferation and cyst formation of cells isolated from a patient with autosomal polycystic kidney disease (Joly et al., 2003) and adhesion and migration of Madin-Darby canine kidney cells (Mak et al., 2006; Moyano et al., 2010; Greciano et al., 2012). These in vitro data also support the idea that LM-332 is a preferred ligand for integrin $\alpha 3\beta 1$ signaling in renal tubule development, maintenance, and recovery from injury (Joly et al., 2003, 2006).

We report that integrin $\alpha 3\beta 1$ primarily regulates Akt and p38 signaling, as activation of these two pathways was diminished in the developing UB of $\text{Hoxb7Cre};\text{Itg}\alpha 3^{\text{lox/lox}}$ mice and when $\text{Itg}\alpha 3^{-/-}$ CD cells were plated on LM-332 and LM-511. These data contrast with the $\text{Hoxb7Cre};\text{Itg}\beta 1^{\text{lox/lox}}$ mice and $\text{Itg}\beta 1^{-/-}$ CD cells, where phosphorylation of FAK and ERK1/2, as well as of Akt and p38, was severely affected (Zhang et al., 2009). Our results suggest that integrins other than $\alpha 3\beta 1$ play additional roles in UB development and that specific $\beta 1$ -containing integrins regulate the precision of signaling in the kidney collecting system.

We show that integrin $\alpha 3\beta 1$ -LM-332 interactions induce Akt activation by mechanisms that are independent of PI3K, Src, and PDK1, but dependent on PTEN and K63 polyubiquitination (Figure 10). Our data suggest that PTEN is responsible for the low basal levels of PIP₃ and Akt activity in $\text{Itg}\alpha 3^{\text{fl/fl}}$ cells, which dramatically increase upon integrin $\alpha 3\beta 1$ binding to LM-332, while we observe opposite effects in $\text{Itg}\alpha 3^{-/-}$ CD cells under the same conditions. These results are consistent with previous studies demonstrating

p85 resulted in marked decrease in phospho-Akt^{Thr308} (D). Adhesion and migration were evaluated as described in *Materials and Methods*. Mean measurements \pm SEM of three independent experiments are shown. (E and F) $\text{Itg}\alpha 3^{\text{fl/fl}}$ and $\text{Itg}\alpha 3^{-/-}$ CD cells were plated on LM-332 (1 $\mu\text{g}/\text{ml}$) as described in Figure 4A. PIP₃ levels were detected using the PIP₃ Mass ELISA Kit as described in *Materials and Methods*. Mean measurements \pm SEM of three independent experiments are shown; *, $p \leq 0.05$ between $\text{Itg}\alpha 3^{\text{fl/fl}}$ and $\text{Itg}\alpha 3^{-/-}$ CD cells (E). Cell lysates (20 μg total protein/lane) were analyzed by Western blotting for levels of total PTEN and phosphorylated and total Src and PDK1 (20 μg total protein/lane) (F). Levels of phosphorylated and total proteins were evaluated as described in Figure 4A. Values are the means \pm SEM of three independent experiments; *, $p \leq 0.05$ between $\text{Itg}\alpha 3^{\text{fl/fl}}$ and $\text{Itg}\alpha 3^{-/-}$ CD cells.

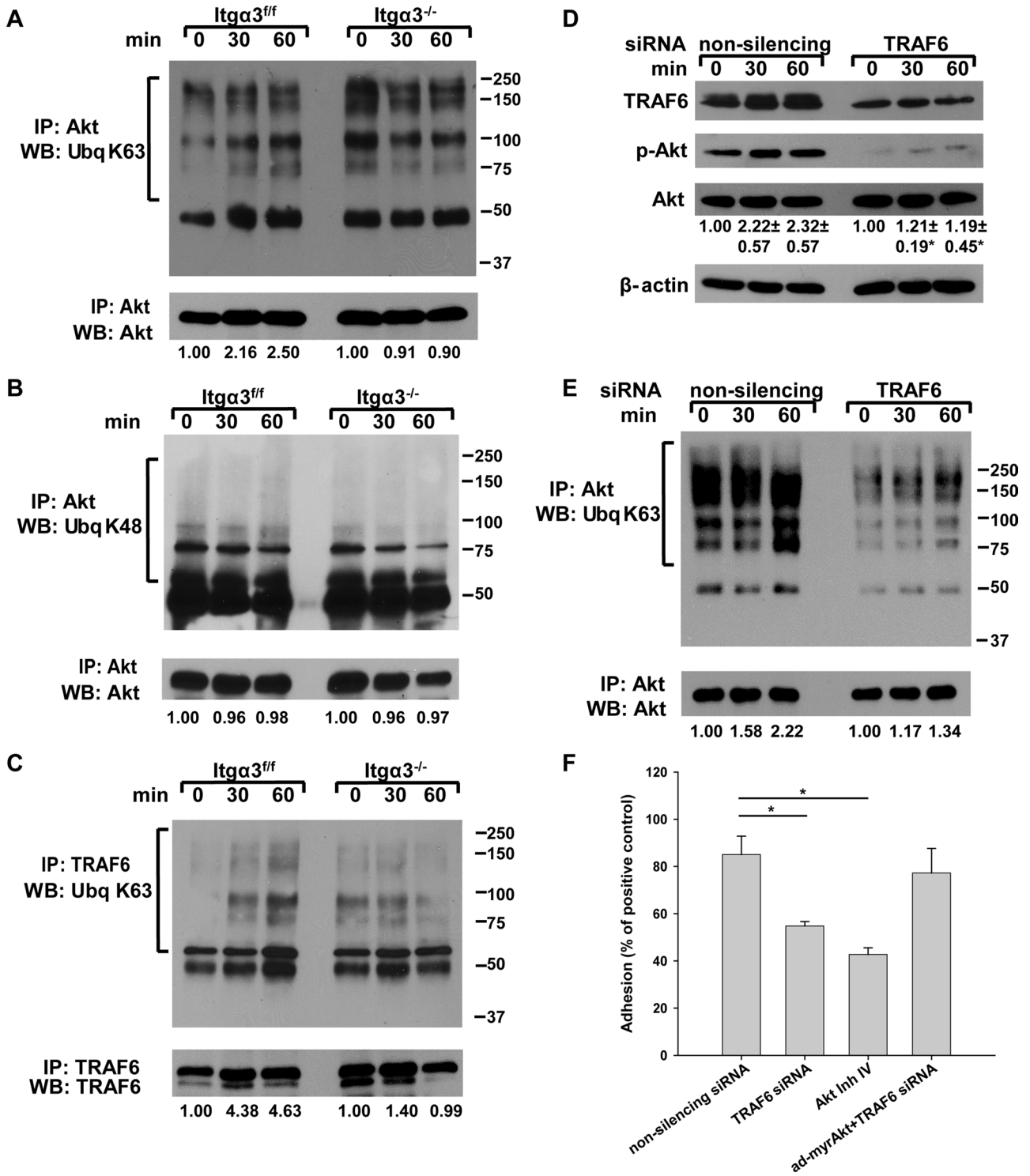


FIGURE 7: Akt activation by integrin α 3 β 1 is regulated by TRAF6-dependent K63-linked polyubiquitination. (A–C) Itg α 3^{ff} and Itg α 3^{-/-} CD cells were plated on LM-332 (1 μ g/ml) as described in Figure 4A. Cell lysates (100 μ g total protein) were immunoprecipitated with anti-Akt antibodies and immunoblotted for K63-linked ubiquitination and Akt (A) or K48-linked ubiquitination and Akt (B). Cell lysates (100 μ g total protein) were immunoprecipitated with antibodies to TRAF6 and immunoblotted for K63 ubiquitination or TRAF6 (C). Levels of ubiquitinated proteins were measured by densitometry, normalized to total protein, and expressed as fold change relative to cells left in suspension (0 time point). A representative of three experiments with quantification at the bottom is shown. (D and E) Itg α 3^{ff} CD cells were transfected with nonsilencing or TRAF6 siRNA (20 nM for 48 h) and subjected to the replating assay on LM-332 (1 μ g/ml). Cell lysates (40 μ g total protein/lane) were immunoblotted for TRAF6, phospho-Akt^{Ser473}, and Akt (D). Levels of phosphorylated and total proteins were evaluated as described in Figure 4A. Values are the means \pm SEM of three independent experiments; *, $p \leq 0.05$ between cells transfected with nonsilencing and TRAF6 siRNA. The same cell lysates (200 μ g total protein) were immunoprecipitated with antibodies to Akt and immunoblotted for K63-linked

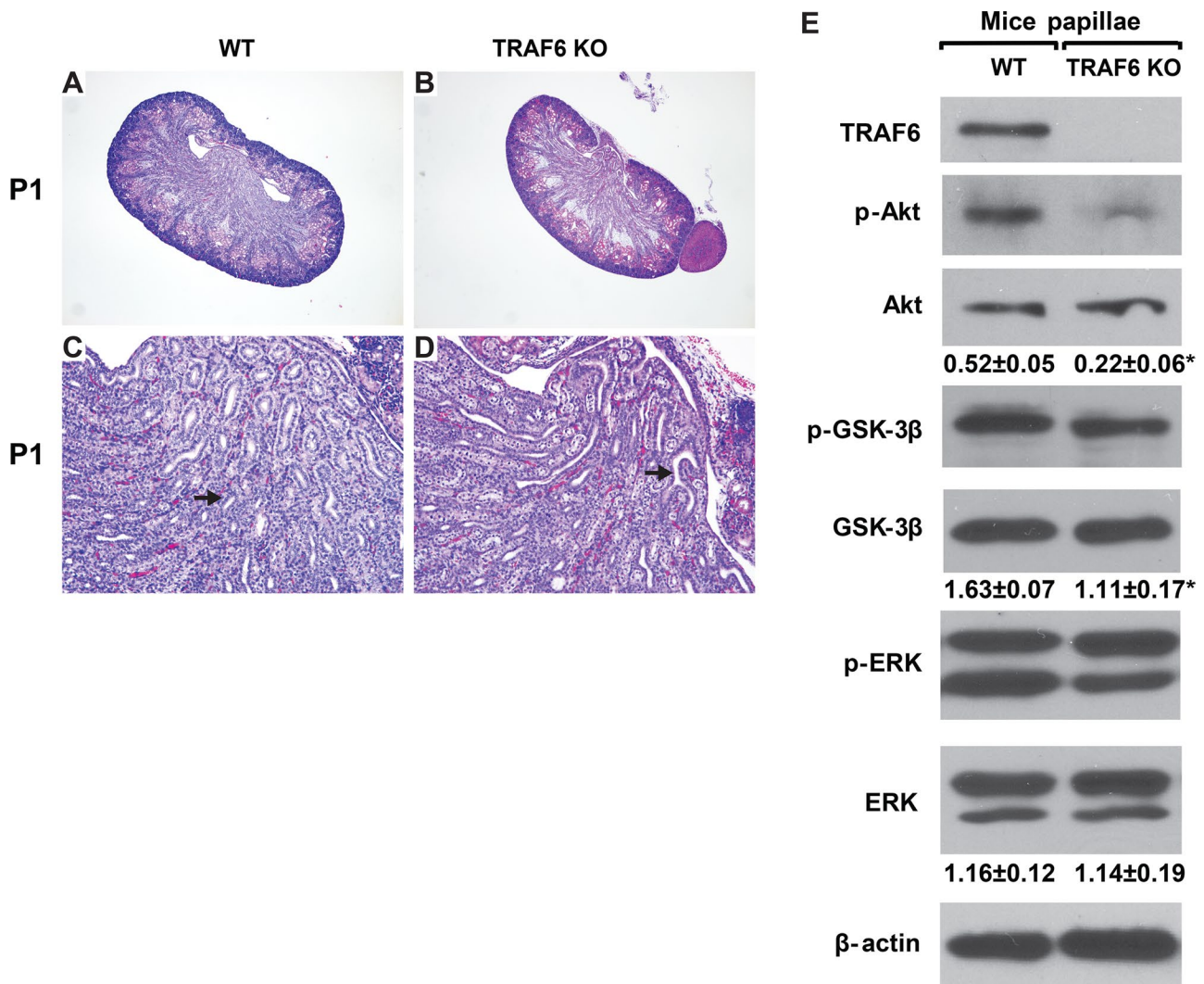


FIGURE 8: TRAF6 KO mice have defective UB development and decreased activation of Akt signaling. (A–D) H&E stained kidneys of newborn (P1), WT mice (TRAF6 WT), and TRAF6-deficient mice (TRAF6 KO). Magnification 40× (A and B) and 100× (C and D). Note the mild branching defect and hypoplastic papilla in the TRAF6 KO mice (arrows). (E) Lysates of papillae from newborn WT and TRAF6 KO mice (20 μg total protein) were analyzed by Western blotting for levels of TRAF6, phospho-Akt^{Ser473}, and phospho-GSK-3β. β-actin was used as a loading control. The amount of phosphorylated proteins was evaluated as in Figure 2. *, $p \leq 0.05$ between WT and TRAF6 KO mice.

that the collagen-binding β1 integrins can regulate PTEN expression in fibroblasts (Xia *et al.*, 2008; Nho and Kahn, 2010), which suggests that this might be a generalized mechanism whereby β1 integrin regulates Akt activation. It is yet to be determined how integrin α3β1 regulates PTEN in CD cells.

We demonstrate that K63-linked polyubiquitination is a novel mechanism whereby integrin α3β1–LM-332 interactions induce Akt activation (Figure 10). These results are consistent with the observations that TRAF6-dependent K63-linked polyubiquitination assists in

Akt translocation to the membrane and is essential for Akt activating phosphorylation following growth factor and cytokine stimulation (Yang *et al.*, 2009, 2010). We also show that TRAF6 regulates integrin α3β1–dependent signaling. TRAF6 E3 ligase activity was increased upon integrin α3β1–dependent adhesion to LM and it was required for Akt activating phosphorylation and cell adhesion to LM. These data are consistent with evidence that TRAF6 K63-linked autopolyubiquitination is the regulatory mechanism for TRAF6 activation and that TRAF6-dependent K63-linked polyubiquitination is a

polyubiquitination or Akt (E). Changes in protein ubiquitination were evaluated as described in A. A representative of three experiments with quantification at the bottom is shown. (F) Itgα3^{fl/fl} CD cells were transfected with nonsilencing or TRAF6 siRNA (20 nM for 48 h), or treated with Akt inhibitor IV (5 μM for 1 h), and/or transduced with ad-myrAkt (100 plaque-forming units/cell for 24 h) and subjected to adhesion assay. Adhesion was evaluated as described in *Materials and Methods*. Mean measurements ± SEM of three independent experiments are shown; *, $p \leq 0.05$ between cells transfected with nonsilencing and TRAF6 siRNA or treated with the Akt inhibitor IV.

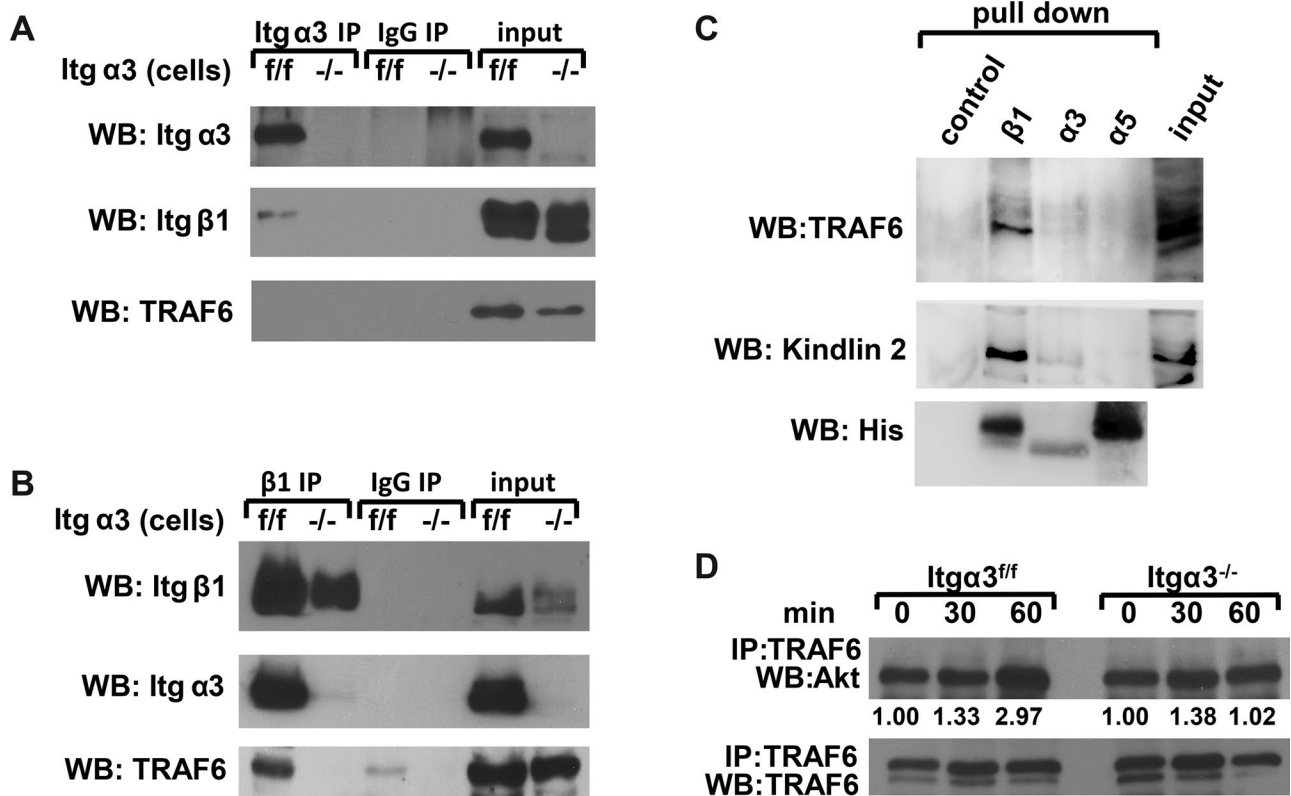


FIGURE 9: TRAF6 forms a complex with α 3 β 1 integrin and Akt. (A and B) Cell lysates from Itg α 3^{f/f} and Itg α 3^{-/-} CD cells (1.0 mg total protein) were immunoprecipitated with protein G-Sepharose-coupled antibody to α 3 (A) or β 1 (B) integrin subunits. Immunoprecipitates were subjected to Western blot analysis with antibodies to TRAF6 or α 3 or β 1 integrin subunits. Input was 20 μ g total protein lysates (2%). (C) Ni-NTA magnetic agarose beads (control), α 3-TM-Cyto domains, α 5-TM-Cyto domains, or β 1-TM-Cyto domains bound to Ni-NTA magnetic agarose beads were incubated with Itg α 3^{f/f} cell lysates and then immunoblotted with antibodies to TRAF6, kindlin 2, or His. (D) Itg α 3^{f/f} and Itg α 3^{-/-} CD cells were trypsinized and replated on LM-332 (1 μ g/ml) as described in Figure 4A. Cell lysates (200 μ g total protein) were immunoprecipitated with antibodies to TRAF6 and immunoblotted for Akt or TRAF6. Levels of Akt and TRAF6 were measured by densitometry, normalized to TRAF6 levels, and expressed as fold change relative to cells left in suspension (0 time point). Values shown are representative of three experiments.

key requirement for Akt activation downstream of other receptors such as the TNF α receptor (Chen, 2012). Our *in vivo* data from TRAF6 KO mice confirm that the regulatory role of TRAF6 for Akt activity in the renal collecting system is associated with developmental abnormalities. Thus it is plausible that our *in vitro* mechanism delineating that α 3 β 1 integrin controls TRAF6-dependent K63-linked polyubiquitination of Akt (Figure 10) explains the phenotype of the Hoxb7Cre;Itg α 3^{flox/flox} mice.

Finally, we found that TRAF6 is present in integrin β 1 immunoprecipitates from Itg α 3^{f/f} but not Itg α 3^{-/-} CD cells and that this interaction is independent of integrin α 3 β 1 binding to ligand. Affinity chromatography with free integrin tails showed that TRAF6 binds only to the integrin β 1 but not the α 3 cytoplasmic tail. These data suggest that, although the TRAF6/ α 3 β 1 integrin complex forms through an interaction of TRAF6 and the β 1 integrin subunit in CD cells, the α 3 integrin subunit is required. These data may explain the interesting observation that there were increased basal levels of Akt activating phosphorylation, Akt K63-linked polyubiquitination, and TRAF6 K63-linked polyubiquitination in Itg α 3^{-/-} compared with Itg α 3^{f/f} CD cells. We speculate that, in Itg α 3^{-/-} CD cells, integrin α 3 β 1 does not interact with TRAF6 and therefore cannot alter its activity. By contrast, in cells expressing the α 3 integrin subunit, integrin α 3 β 1 acts as a repressor of TRAF6 activity when the integrin is

not bound to LM. After the cells adhere to LM, TRAF6 is activated in an integrin-dependent manner by mechanisms that are yet to be determined.

In conclusion, this study demonstrates that integrin α 3 β 1 interactions with both α 3- and α 5-containing LMs regulate UB development by functionally modulating the Akt signaling pathway. In addition, we show that K63-linked polyubiquitination plays a previously unrecognized role in integrin α 3 β 1-dependent cell signaling required for UB development and that this may be a novel general mechanism whereby integrins regulate signaling pathways.

MATERIALS AND METHODS

Reagents, adenovirus vectors, siRNAs, and antibodies

Human laminin 332 (LM-332) was produced, purified, and evaluated as previously described (Tripathi *et al.*, 2008). LM-111 was produced as previously described (McKee *et al.*, 2007, 2009). Collagen I was purchased from BD Biosciences (San Jose, CA); fibronectin and vitronectin were purchased from Sigma-Aldrich (St. Louis, MO). Akt inhibitor IV, PI3K inhibitor LY294002, and p38 inhibitor SB203580 were purchased from Calbiochem (San Diego, CA).

LM-511 was produced as a heterotrimer of mouse LM α 5, hemagglutinin (HA)-tagged human LM β 1, and human LM γ 1, as

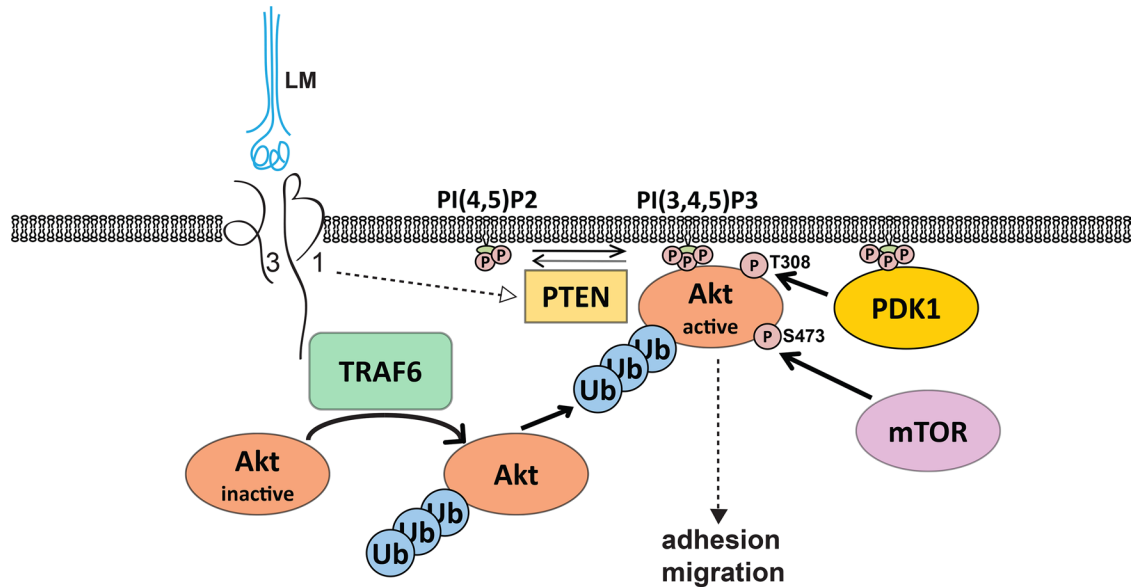


FIGURE 10: LM-332/integrin $\alpha 3\beta 1$ interactions induce Akt activation by TRAF6-mediated K63-linked polyubiquitination. Integrin $\alpha 3\beta 1$ interactions with LM induce the formation of a TRAF6/ $\alpha 3\beta 1$ integrin complex through binding of TRAF6 to the cytoplasmic tail of $\beta 1$ integrin subunit. This complex is required for TRAF6 activation and triggers K63-linked polyubiquitination of Akt, which facilitates Akt translocation to the cellular membrane. Integrin $\alpha 3\beta 1$ interactions with LM also induce PTEN inactivation that results in an increase of PIP₃ and Akt anchoring to the membrane, where it is phosphorylated and fully activated.

previously described (McKee *et al.*, 2007). The complete mouse LM $\alpha 5$ cDNA in an LZ10 plasmid (kindly provided by Jeffrey Miner, Washington University, St. Louis, MO) was excised with *EcoR1* and ligated into the expression vector pcDNA3.1 puro. HEK293 cells stably expressing the human $\beta 1$ LM subunit containing an N-terminal HA tag and the $\gamma 1$ LM subunit (McKee *et al.*, 2007, 2009) were transfected with the LM $\alpha 5$ construct. Stable clones secreting the LM into media were selected and expanded. Recombinant LM-511 protein was purified by affinity chromatography from conditioned medium of HEK293 cells on an HA matrix (E6779; Sigma-Aldrich) and eluted per manufacturer's conditions with 0.1 M glycine (pH 2.8). Protein was concentrated in Amicon ultra 15 filters (100K mwco, ufc900024; Millipore, Billerica, MA) and dialyzed in 50 mM Tris (pH 7.4), 90 mM NaCl, and 0.125 mM EDTA. The homogeneity of purified LM-511 was confirmed by Coomassie blue staining of SDS-PAGE (Supplemental Figure 1A). The correct folding of LM-511 was confirmed by a polymerization assay (Supplemental Figure 1B; McKee *et al.*, 2007), and LM-511 activity was assessed by binding with recombinant $\alpha 7\beta 1$ and $\alpha 6\beta 1$ integrins (Supplemental Figure 1C; McKee *et al.*, 2012).

Adenoviruses with vectors encoding GFP, ad-GFP, the dominant-negative catalytic subunit deletion mutant PI3K, ad-delta p85, and constitutively active myristoylated Akt (ad-myrAkt) were propagated in HEK293 cells, purified by column chromatography, quantitated, and used for cell infection based on particle yield as previously described (Tan *et al.*, 2006).

SignalSilence Akt siRNA I (sequence [5'-3'] UGCCCCUUCUACAACCAGGA) and SignalSilence Akt1 siRNA I (mouse-specific, sequence [5'-3'] GCUCAAGAAGGACCCUACA) were purchased from Cell Signaling Technology (Danvers, MA). Silencer Select predesigned TRAF6 siRNAs (sequences [5'-3'] CAUUAAGGAUGAUACAUUAtt and AGAAAAGAGUUGUAGUUUUtt) and Silencer Select Negative control #1 siRNA were bought from Ambion (Carlsbad, CA).

The following antibodies were used in Western immunoblot analyses: integrin $\alpha 3$ (AB1920 [Millipore, Temecula, CA] and AF2787 [R&D Systems]); integrin $\beta 1$ (AB1952; Millipore); integrin $\beta 4$ (AF4054; R&D Systems); integrin $\alpha 6$ (3750), phospho-Akt^{Thr308} (9275), phospho-Akt^{Ser473} (9271), total Akt (9272), phospho-GSK-3 β ^{Ser9} (9322), total GSK-3 β (9315), phospho-p38^{Thr180/Tyr182} (9211), total p38 (9212), phospho-ERK1/2^{Thr202/Tyr204} (9101), total ERK1/2 (9102), phospho-PDK1^{Ser241} (3438) and total PDK1 (5662), phospho-Src^{Tyr416} family (2101), total Src (2108), PTEN (9552), K48-linkage specific polyubiquitin (8081), and K63-linkage specific polyubiquitin (5621) (all from Cell Signaling Technologies); TRAF6 (ab94720; Abcam, Cambridge, MA); kindlin 2 (MAB2617; Millipore); and His (620-0203; Bio-Rad). Antibodies for TRAF6 (H-274; Santa Cruz Biotechnology), Akt (4685; Cell Signaling), integrin $\beta 1$ (MAB1997; Millipore), integrin $\alpha 3$ (AF2787; R&D Systems), and integrin $\alpha 6$ (H-87; Santa Cruz Biotechnology) were used for immunoprecipitation. Antibody to β -actin (A4700, Sigma-Aldrich) was used to evaluate protein loading. Anti-mouse $\beta 1$ (550530), $\alpha 1$ (555001), $\alpha 2$ (553819), $\alpha 5$ (553350), $\alpha 6$ (555734), and $\alpha \nu$ (550024) integrin antibodies were purchased from BD Biosciences. R-phycoerythrin-conjugated secondary antibodies were purchased from Invitrogen (Carlsbad, CA). Antibodies to integrin $\alpha 6$ (555734; BD Biosciences) were used in adhesion assays.

Laminin subunits $\alpha 3$ and $\gamma 2$ global knockout mice

All animal experiments were approved by the Vanderbilt University Institutional Animal Use and Care Committee. LM $\alpha 3$ global knockout mice were kindly provided by W. Carter (University of Washington; Ryan *et al.*, 1999). LM $\gamma 2$ knockout mice were a gift from J. Uitto (Thomas Jefferson University; Meng *et al.*, 2003).

TRAF6-deficient mice

Generation of the global TRAF6 KO mice on 129SV background was previously described (Naito *et al.*, 1999). The genotyping was verified by PCR amplification of the genomic DNA with the

following primers: forward primer, 5'-CGTGCCATGTAATGCA-TTCTG-3'; reverse primer, 5'-CGAGATGTCTCAGTTCCATC-3'; and reverse mutant primer to amplify the TRAF6 gene deleted sequence, 5'-CACTCAGCACCATTTCCTAACCT-3'. Mice were bred as heterozygotes, and age-matched WT and TRAF6 KO littermates were used in experiments.

Generation of HoxB7Cre:Itg α 3^{fllox/fllox} mice

Integrin α 3^{fllox/fllox} (Itg α 3^{fllox/fllox}) mice (Sachs *et al.*, 2006), were crossed with the HoxB7Cre mice (generous gift of A. McMahon, University of Southern California; Kobayashi *et al.*, 2005). Age-matched littermates homozygous for the integrin Itg α 3^{fllox/fllox} gene, but lacking Cre (Itg α 3^{fllox/fllox} mice), were used as controls. The expression of integrin α 3 and activation of signaling pathways in the developing mouse CDs was determined using Western immunoblot analysis.

Western blot analysis

Papillae from individual 3-d-old pups were isolated and lysed using a Polytron homogenizer in T-PER reagent (Thermo Scientific, Waltham, MA) with protease inhibitors and phosphatase inhibitors cocktail 1 and 2 (Sigma-Aldrich). Cell lysates were prepared using M-PER reagent (Thermo Scientific). Lysates were centrifuged at 17,000 \times g for 15 min at 4°C, and total protein concentration was determined using BCA reagent (Thermo Scientific). Protein extracts were subjected to Western immunoblot analysis and developed using the Western Lightning Chemiluminescence Plus detection system (Perkin Elmer-Cetus, Wellesley, MA) according to the manufacturer's protocol. Densitometry was performed using the ImageJ program. For quantification of levels of protein phosphorylation, OD of bands for phosphoprotein was normalized to total protein and β -actin.

Morphological and immunohistochemical analysis

Whole mouse embryos or kidneys were removed, fixed, stained with hematoxylin and eosin (H&E) and evaluated by light microscopy as previously described (Mathew *et al.*, 2012). For analysis of LM-332 expression, tissue sections were treated with antigen-retrieval citra buffer for 10 min, blocked with 5% normal goat serum in phosphate-buffered saline (PBS) for 1 h at room temperature, and incubated with primary rabbit anti-rat LM γ 2 antibody (Giannelli *et al.*, 1999). After incubation with biotinylated anti-rabbit antibody for 1 h at room temperature, LM332 was visualized using ABC reagent (a preformed avidin/biotinylated enzyme complex that was developed with 3,3'-diaminobenzidine horseradish peroxidase substrate). Slides were counterstained with hematoxylin. Similarly, tissue sections were probed with rabbit anti-rat LM α 3 antibody (M3.3). Ki67 staining and scoring was performed as previously described (Mathew *et al.*, 2012).

Generation of integrin α 3^{-/-} CD cells

CD cells were isolated from 5- to 6-wk-old Itg α 3^{fllox/fllox} mice as described by Husted *et al.* (1988) and immortalized with pSV40 plasmid. Loci for the α 3 integrin subunit in CD cells were deleted with adenovirus expressing Cre recombinase. CD cells were grown in DMEM/F12 containing 10% fetal bovine serum and 1% penicillin/streptomycin.

Flow cytometry analysis

Flow cytometry analysis was performed as previously described (Zhang *et al.*, 2009). CD cells were incubated with anti-mouse β 1, β 4, α 1, α 2, α 6, and α v integrin antibodies followed by fluorescein isothiocyanate-conjugated secondary antibodies.

Cell adhesion

Cell adhesion assays were performed in 96-well plates as previously described (Chen *et al.*, 2004). Cells (1×10^5) were seeded in serum-free medium onto plates containing different concentrations of ECM for 60 min. Nonadherent cells were removed; the remaining cells were fixed, stained with crystal violet, and solubilized; and the optical densities of the cell lysates were read at 570 nm (OD₅₇₀). Adhesion was calculated as percent of positive control (adhesion to serum).

Cell migration

Cell migration was assayed as previously described (Chen *et al.*, 2004). Transwells with 8- μ m pores were coated with different ECM components, and 1×10^5 cells were added to the upper well in serum-free medium. Cells that migrated through the filter after 4 h were counted.

Cell proliferation

Cell proliferation was assessed by measuring incorporation of 5-bromodeoxyuridine (BrdU) in an enzyme-linked immunosorbent assay-based 5-Bromo-2'-deoxy-uridine Labeling and Detection Kit III (Roche Applied Science, Indianapolis, IN) as previously described (Linkous *et al.*, 2010). BrdU incorporation was quantified by a change of absorbance (OD) at 405 nm.

Cell replating assays

Cell replating assays were performed on CD cells that were trypsinized, washed, suspended in serum-free DMEM, plated on LM-332 or LM-511 (1 μ g/ml), and harvested 0, 30, and 60 min later. Cells were washed in PBS and lysed using M-PER reagent with protease and phosphatase inhibitor cocktails (Sigma-Aldrich). Protein extracts (20–40 μ g) were subjected to Western immunoblot analysis.

When chemical inhibitors were used, they were added 1 h before the assays. Adenoviral infection of cells was performed at 10–100 plaque-forming units/cell as previously described (Tan *et al.*, 2006), and the assays were performed 24 h later. For silencing experiments, cells were transfected with nonsilencing siRNA (20 nM, transfection control) or Akt siRNA (100 nM) or TRAF6 siRNA (20 nM) using Lipofectamine RNAiMAX according to the manufacturer's instructions. Transfected cells were used 48 h later.

Evaluation of PIP₃ levels

CD cells were subjected to the replating assay using 150-mm cell culture plates coated with LM-332 (1 mg/ml) and were harvested at 0, 30, and 60 min after plating. Lipids were extracted using a modified Bligh and Dyer method as previously described (Yazlovitskaya *et al.*, 2008). PIP₃ levels were detected using the PIP₃ Mass ELISA Kit (Echelon, Salt Lake City, UT) according to the manufacturer's instructions.

Immunoprecipitation

For immunoprecipitation, antibody or corresponding normal immunoglobulin G (IgG) were covalently bound to protein A/G Sepharose (Thermo Scientific) as previously described (Persons *et al.*, 1999). Immunoprecipitations were performed with 0.1 mg (for integrin α 6), 0.2 mg (for Akt and TRAF6), or 1.0 mg (for integrins α 3 or β 1) of total cell lysates overnight at 4°C with rotating, after which the bound immune complexes were washed, resuspended in SDS-PAGE sample buffer, heated at 95°C for 10 min, cleared by centrifugation, and subjected to Western immunoblot analysis. For immunoprecipitation of integrins α 3 or β 1, cells were grown on uncoated cell culture surfaces where integrin α 3 β 1 is not ligated by ligand.

Pull-down assay

N-terminally 6xHis-tagged integrin β 1-TM-Cyto (transmembrane-cytoplasmic domains, mouse residues from 719 to 798 of the full-length protein), α 5-TM-Cyto (mouse residues from 993 to 1053 of the full-length protein), and α 3-TM-Cyto (mouse residues from 991 to 1053 of the full-length protein) were cloned into a pET15b vector and transformed into BL21 (DE3) Arctic Express *Escherichia coli*. After protein induction with 1 mM isopropyl β -D-1-thiogalactopyranoside, cells were pelleted by centrifugation, resuspended in TBS buffer (Tris 50 mM, NaCl 150 mM, pH 7.4) with 100 μ g/ml lysozyme and 50 μ g/ml DNase, and rotated at 4°C for 2 h. Cell lysates were treated with Empigen (30% solution; 1 ml per 10 ml of lysate) at 4°C for 1 h with rotation and centrifuged. Supernatants were incubated with Ni-NTA magnetic agarose beads (Qiagen) at 4°C for 3 h, washed three times with TBS buffer, and incubated with CD cell lysates (lysis buffer: 1% NP40, Tris 50 mM, NaCl 150 mM, pH 7.4, protease inhibitor cocktail [Sigma-Aldrich]) overnight at 4°C. After three washes with lysis buffer, proteins were eluted from the beads by being boiled with 80 μ l SDS-PAGE sample buffer for 5 min and were subjected to Western blot analyses with antibodies to TRAF6, kindlin 2, or His.

Statistical analyses

The mean and SEM of each treatment group were calculated for all experiments. At least four independent experiments (some in triplicates each) were performed. Student's *t* test was used to compare two groups. All statistical tests were two-sided, and statistical analysis was done with the use of SigmaStat software (Systat Software, San Jose, CA). Statistical significance was defined as $p \leq 0.05$.

ACKNOWLEDGMENTS

We thank William Carter for the LM α 3-null mice and Jouni Uitto for the LM γ 2-null mice. We thank Catherine Alford for her technical help with cell sorting and flow cytometry and Reinhard Fassler and Marc Schmidt-Suppran for constructive criticism of the project. This work was supported by VA Merit Review 1101BX002025 (Ambra Pozzi [A.P.]) and 1101BX002196 (R.Z.) and National Institutes of Health Grants R01-CA162433 (A.P.), R01-DK095761 (A.P.), R01-DK083187 (R.Z.), R01-DK075594 (R.Z.), R01-DK066921 (R.Z.), and R01-DK36425 (P.Y.). A.S. is supported by the Netherlands Kidney Foundation. H.-Y.T. and R.T.B. are supported by the Max Planck Society and the Deutsche Forschungsgemeinschaft (DFG; SFB 914).

REFERENCES

Aumailley M, Bruckner-Tuderman L, Carter WG, Deutzmann R, Edgar D, Ekblom P, Engel J, Engvall E, Hohenester E, Jones JC, et al. (2005). A simplified laminin nomenclature. *Matrix Biol* 24, 326–332.

Bayascas JR (2008). Dissecting the role of the 3-phosphoinositide-dependent protein kinase-1 (PDK1) signalling pathways. *Cell Cycle* 7, 2978–2982.

Cantley LC (2002). The phosphoinositide 3-kinase pathway. *Science* 296, 1655–1657.

Chen D, Roberts R, Pohl M, Nigam S, Kreidberg J, Wang Z, Heino J, Ivaska J, Coffa S, Harris RC, et al. (2004). Differential expression of collagen- and laminin-binding integrins mediates ureteric bud and inner medullary collecting duct cell tubulogenesis. *Am J Physiol Renal Physiol* 287, F602–F611.

Chen ZJ (2012). Ubiquitination in signaling to and activation of IKK. *Immunol Rev* 246, 95–106.

Giannelli G, Pozzi A, Stetler-Stevenson WG, Gardner HA, Quaranta V (1999). Expression of matrix metalloproteinase-2-cleaved laminin-5 in breast remodeling stimulated by sex steroids. *Am J Pathol* 154, 1193–1201.

Greciano PG, Moyano JV, Buschmann MM, Tang J, Lu Y, Rudnicki J, Manninen A, Matlin KS (2012). Laminin 511 partners with laminin 332 to mediate directional migration of Madin-Darby canine kidney epithelial cells. *Mol Biol Cell* 23, 121–136.

Guertin DA, Sabatini DM (2007). Defining the role of mTOR in cancer. *Cancer Cell* 12, 9–22.

Husted RF, Hayashi M, Stokes JB (1988). Characteristics of papillary collecting duct cells in primary culture. *Am J Physiol* 255, F1160–F1169.

Jiang T, Qiu Y (2003). Interaction between Src and a C-terminal proline-rich motif of Akt is required for Akt activation. *J Biol Chem* 278, 15789–15793.

Joly D, Berissi S, Bertrand A, Strehl L, Patey N, Knebelmann B (2006). Laminin 5 regulates polycystic kidney cell proliferation and cyst formation. *J Biol Chem* 281, 29181–29189.

Joly D, Morel V, Hummel A, Ruello A, Nusbaum P, Patey N, Noel LH, Rouselle P, Knebelmann B (2003). β 4 integrin and laminin 5 are aberrantly expressed in polycystic kidney disease: role in increased cell adhesion and migration. *Am J Pathol* 163, 1791–1800.

Kobayashi A, Kwan KM, Carroll TJ, McMahon AP, Mendelsohn CL, Behringer RR (2005). Distinct and sequential tissue-specific activities of the LIM-class homeobox gene *Lim1* for tubular morphogenesis during kidney development. *Development* 132, 2809–2823.

Kreidberg JA, Donovan MJ, Goldstein SL, Rennke H, Shepherd K, Jones RC, Jaenisch R (1996). Alpha 3 beta 1 integrin has a crucial role in kidney and lung organogenesis. *Development* 122, 3537–3547.

Lamothe B, Besse A, Campos AD, Webster WK, Wu H, Darnay BG (2007). Site-specific Lys-63-linked tumor necrosis factor receptor-associated factor 6 auto-ubiquitination is a critical determinant of I kappa B kinase activation. *J Biol Chem* 282, 4102–4112.

Landstrom M (2010). The TAK1-TRAF6 signalling pathway. *Int J Biochem Cell Biol* 42, 585–589.

Linkous AG, Yazlovitskaya EM, Hallahan DE (2010). Cytosolic phospholipase A2 and lysophospholipids in tumor angiogenesis. *J Natl Cancer Inst* 102, 1398–1412.

Liu Y, Chattopadhyay N, Qin S, Szekeres C, Vasylyeva T, Mahoney ZX, Tagliente M, Bates CM, Chapman HA, Miner JH, Kreidberg JA (2009). Coordinate integrin and c-Met signaling regulate *Wnt* gene expression during epithelial morphogenesis. *Development* 136, 843–853.

Lomaga MA, Henderson JT, Elia AJ, Robertson J, Noyce RS, Yeh WC, Mak TW (2000). Tumor necrosis factor receptor-associated factor 6 (TRAF6) deficiency results in exencephaly and is required for apoptosis within the developing CNS. *J Neurosci* 20, 7384–7393.

Lomaga MA, Yeh WC, Sarosi I, Duncan GS, Furlonger C, Ho A, Morony S, Capparelli C, Van G, Kaufman S, et al. (1999). TRAF6 deficiency results in osteopetrosis and defective interleukin-1, CD40, and LPS signaling. *Genes Dev* 13, 1015–1024.

Mak GZ, Kavanaugh GM, Buschmann MM, Stickley SM, Koch M, Goss KH, Waechter H, Zuk A, Matlin KS (2006). Regulated synthesis and functions of laminin 5 in polarized Madin-Darby canine kidney epithelial cells. *Mol Biol Cell* 17, 3664–3677.

Mathew S, Lu Z, Palamuttam RJ, Mernaugh G, Hadziselimovic A, Chen J, Bulus N, Gewin LS, Voehler M, Meves A, et al. (2012). β 1 integrin NPXY motifs regulate kidney collecting-duct development and maintenance by induced-fit interactions with cytosolic proteins. *Mol Cell Biol* 32, 4080–4091.

McKee KK, Capizzi S, Yurchenco PD (2009). Scaffold-forming and adhesive contributions of synthetic laminin-binding proteins to basement membrane assembly. *J Biol Chem* 284, 8984–8994.

McKee KK, Harrison D, Capizzi S, Yurchenco PD (2007). Role of laminin terminal globular domains in basement membrane assembly. *J Biol Chem* 282, 21437–21447.

McKee KK, Yang DH, Patel R, Chen ZL, Strickland S, Takagi J, Sekiguchi K, Yurchenco PD (2012). Schwann cell myelination requires integration of laminin activities. *J Cell Sci* 125, 4609–4619.

Meng X, Klement JF, Leperi DA, Birk DE, Sasaki T, Timpl R, Uitto J, Pulkkinen L (2003). Targeted inactivation of murine laminin γ 2-chain gene recapitulates human junctional epidermolysis bullosa. *J Invest Dermatol* 121, 720–731.

Miner JH, Li C (2000). Defective glomerulogenesis in the absence of laminin α 5 demonstrates a developmental role for the kidney glomerular basement membrane. *Dev Biol* 217, 278–289.

Miner JH, Yurchenco PD (2004). Laminin functions in tissue morphogenesis. *Annu Rev Cell Dev Biol* 20, 255–284.

Moyano JV, Greciano PG, Buschmann MM, Koch M, Matlin KS (2010). Autocrine transforming growth factor- β 1 activation mediated by integrin α v β 3 regulates transcriptional expression of laminin-332 in Madin-Darby canine kidney epithelial cells. *Mol Biol Cell* 21, 3654–3668.

Naito A, Azuma S, Tanaka S, Miyazaki T, Takaki S, Takatsu K, Nakao K, Nakamura K, Katsuki M, Yamamoto T, Inoue J (1999). Severe osteopetrosis, defective interleukin-1 signalling and lymph node organogenesis in TRAF6-deficient mice. *Genes Cells* 4, 353–362.

- Nho RS, Kahm J (2010). β 1-integrin-collagen interaction suppresses FoxO3a by the coordination of Akt and PP2A. *J Biol Chem* 285, 14195–14209.
- Persons DL, Yazlovitskaya EM, Cui W, Pelling JC (1999). Cisplatin-induced activation of mitogen-activated protein kinases in ovarian carcinoma cells: inhibition of extracellular signal-regulated kinase activity increases sensitivity to cisplatin. *Clin Cancer Res* 5, 1007–1014.
- Ryan MC, Lee K, Miyashita Y, Carter WG (1999). Targeted disruption of the LAMA3 gene in mice reveals abnormalities in survival and late stage differentiation of epithelial cells. *J Cell Biol* 145, 1309–1323.
- Sachs N, Kreft M, van den Bergh Weerman MA, Beynon AJ, Peters TA, Weening JJ, Sonnenberg A (2006). Kidney failure in mice lacking the tetraspanin CD151. *J Cell Biol* 175, 33–39.
- Song MS, Salmena L, Pandolfi PP (2012). The functions and regulation of the PTEN tumour suppressor. *Nat Rev Mol Cell Biol* 13, 283–296.
- Tan J, Geng L, Yazlovitskaya EM, Hallahan DE (2006). Protein kinase B/Akt-dependent phosphorylation of glycogen synthase kinase-3 β in irradiated vascular endothelium. *Cancer Res* 66, 2320–2327.
- Tripathi M, Nandana S, Yamashita H, Ganesan R, Kirchofer D, Quaranta V (2008). Laminin-332 is a substrate for hepsin, a protease associated with prostate cancer progression. *J Biol Chem* 283, 30576–30584.
- Wang G, Gao Y, Li L, Jin G, Cai Z, Chao JI, Lin HK (2012). K63-linked ubiquitination in kinase activation and cancer. *Front Oncol* 2, 5.
- Wu H, Arron JR (2003). TRAF6, a molecular bridge spanning adaptive immunity, innate immunity and osteoimmunology. *Bioessays* 25, 1096–1105.
- Xia H, Diebold D, Nho R, Perlman D, Kleidon J, Kahm J, Avdulov S, Peterson M, Nerva J, Bitterman P, Henke C (2008). Pathological integrin signaling enhances proliferation of primary lung fibroblasts from patients with idiopathic pulmonary fibrosis. *J Exp Med* 205, 1659–1672.
- Yang DH, McKee KK, Chen ZL, Mernaugh G, Strickland S, Zent R, Yurchenco PD (2011). Renal collecting system growth and function depend upon embryonic γ 1 laminin expression. *Development* 138, 4535–4544.
- Yang WL, Wang J, Chan CH, Lee SW, Campos AD, Lamothe B, Hur L, Grabiner BC, Lin X, Darnay BG, Lin HK (2009). The E3 ligase TRAF6 regulates Akt ubiquitination and activation. *Science* 325, 1134–1138.
- Yang WL, Wu CY, Wu J, Lin HK (2010). Regulation of Akt signaling activation by ubiquitination. *Cell Cycle* 9, 487–497.
- Yazlovitskaya EM, Linkous AG, Thotala DK, Cuneo KC, Hallahan DE (2008). Cytosolic phospholipase A2 regulates viability of irradiated vascular endothelium. *Cell Death Differ* 15, 1641–1653.
- Zent R, Bush KT, Pohl ML, Quaranta V, Koshikawa N, Wang Z, Kreidberg JA, Sakurai H, Stuart RO, Nigam SK (2001). Involvement of laminin binding integrins and laminin-5 in branching morphogenesis of the ureteric bud during kidney development. *Dev Biol* 238, 289–302.
- Zhang X, Mernaugh G, Yang DH, Gewin L, Srichai MB, Harris RC, Iturregui JM, Nelson RD, Kohan DE, Abrahamson D, *et al.* (2009). β 1 integrin is necessary for ureteric bud branching morphogenesis and maintenance of collecting duct structural integrity. *Development* 136, 3357–3366.